Variable-timing, fixed-rate application of cattle biogas effluent as fertilizer for rice using a leaf color chart

Small-scale biogas production from farmyard manure for domestic usage is popular in Vietnam. However, there are cases when untreated effluents from biogas digesters (i.e., anaerobic digestion effluents), including plant nutrients such as nitrogen (N), are discharged to river systems, causing environmental problems such as water pollution. To solve it, we proposed using the biogas effluent as fertilizer for rice, the major local crop. In practice, farmers need to know N concentration in the effluent to determine the application amount and timing. Although the application amount can be roughly estimated using a test paper for N concentration, the application timing plays the main role in adjusting the deficiency and excess of the estimated amount. Here we examined the performance of variable-timing, fixed-rate application of biogas effluent from cattle manure for rice production (cultivar: OM5451) using a leaf color chart (LCC) that was developed by the International Rice Research Institute (IRRI, Fig. 1). Two microcosm experiments were carried out at a plastic film house in Can Tho, Vietnam, in different seasons in 2018.

We set several LCC threshold values (Table 1), below which we applied a fixed amount of the effluent as illustrated in Figure 2. By each incremental raising of the LCC threshold, the application timing and the resultant total amount were increased (Table 1). There was a positive linear relationship between LCC values and Soil Plant Analysis Development (SPAD) values, an indicator of leaf chlorophyll content, regardless of the seasons (Fig. 3). This relationship indicates that a cheap LCC can substitute for an expensive SPAD meter to estimate leaf color even in the case of using effluent as fertilizer. Rice grain yield and straw biomass were also increased by raising the LCC threshold, suggesting that determining the application timing based on LCC threshold is feasible under microcosm conditions. There were positive linear relationships between the mean LCC values during 21 to 81 days after sowing and the grain yields in both seasons (Fig. 4). The optimum LCC threshold for effluent application was 3.75 under microcosm conditions.

The proposed method can achieve yield levels comparable to those from inorganic fertilizers. However, when determining the application amount based on N concentration in the effluent, the application amounts of phosphorus (P) and potassium (K) from the effluent may become deficient or excessive due to the imbalance of NPK concentrations. The optimum LCC threshold in terms of rice grain yield may change depending on the cultivar and environment, therefore farmers need to determine it independently. Because the use of effluent as fertilizer requires additional labor and cost compared to that of inorganic fertilizers, financial administrative support is essential in order to mitigate the environmental problems.

(K. Minamikawa, Y. Hosen [Institute for Agro-Environmental Sciences, NARO, Japan], C.K. Huynh [Can Tho University, Vietnam (CTU)], S.N. Tran [CTU], H.C. Nguyen [CTU])

Table 1. The method and the total rate (kg N ha^{-1}) of N application for eight treatments in two experiments

Treatment	Application method	Experiment 1	Experiment 2
Zero	No nitrogen	0	0
Estd	Split-application, for three times at conventional timings	150 (30-50-70)	150 (30-50-70)
E2.75	60 kg N ha^{-1} as effluent whenever LCC value goes below 2.75	90 (30-60)	90 (30-60)
E3.00	60 kg N ha^{-1} as effluent whenever LCC value goes below 3.00	90 (30-60)	90 (30-60)
E3.25	60 kg N ha^{-1} as effluent whenever LCC value goes below 3.25	90 (30-60)	90 (30-60)
E3.50	60 kg N ha^{-1} as effluent whenever LCC value goes below 3.50	150 (30-60-60)	150 (30-60-60)
E3.75	60 kg N ha^{-1} as effluent whenever LCC value goes below 3.75	150 (30-60-60)	210 (30-60-60-60)
U3.25	60 kg N ha^{-1} as urea whenever LCC value goes below 3.25	150 (30-60-60)	90 (30-60)

Experiment 1 mainly in dry season and Experiment 2 mainly in wet season.

The first N application was conducted 10 or 11 days after sowing at 30 kg N ha^{-1}, except for Zero treatment.

P and K (only in Zero and U3.25 treatments) were split-applied as inorganic fertilizers at conventional timings.

Fig. 1. Measuring the LCC value

(Photo courtesy: Mr. Ariel Javellana, IRRI)

Fig. 2. An example of seasonal shifts in LCC values in Experiment 2

Arrows indicate the timings of N application in respective treatments. Grey shade indicates the target period for N application.

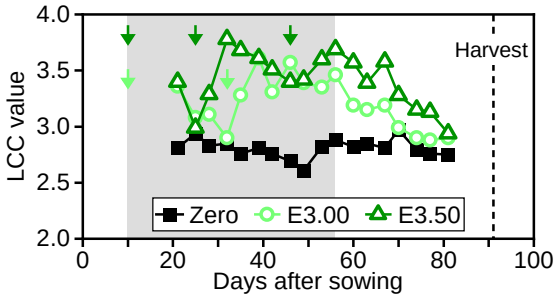

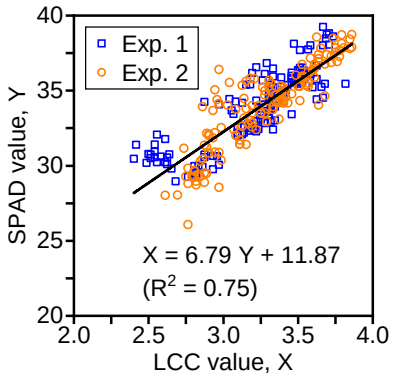

Fig. 3. Relationship between LCC values and SPAD values in two experiments

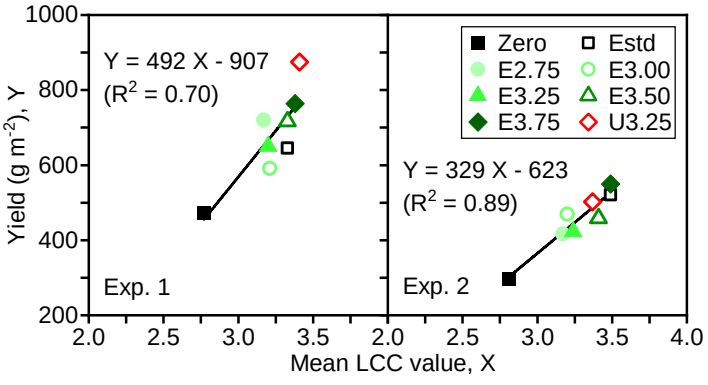

Fig. 4. Relationships between the mean LCC values and rice grain yields in two experiments

Yield is expressed as 14% moisture content.

Oxygenation of flooded paddy soil and inhibition of methane production through irrigation with water containing bulk oxygen nanobubbles

Rice cultivation is one of the major anthropogenic sources of methane (CH_4), a potent greenhouse gas. Methane is produced in flooded paddy soils under reductive conditions, thus surface water drainage, such as midseason drainage and alternate wetting and drying (AWD), is effective in reducing CH_4 emission through soil oxidation. However, the feasibility of drainage practices is limited spatiotemporally in wet seasons and lowlands with poor drainage. To reduce CH_4 emission from flooded paddy soils, we proposed an irrigation scheme using water containing bulk nanobubbles (NBs) (Minamikawa et al. 2015). NBs are tiny bubbles (<1 μm diameter) made of various gases that have unique properties including a long lifetime in water. We had demonstrated that oxygen NB water (i.e., water with NBs made of pure oxygen) significantly reduced the direct CH_4 emission by 21% in a pot experiment, but the mechanisms underlying the emission reduction had remained unclear. This study hypothesized that the emission reduction is caused by the oxygenation of flooded soil through the leaching of oxygen NB water. To test it, we carried out three soil-column experiments using a Fluvisol under flooded and rice-unplanted conditions (Fig. 1).

Oxygen NB water prepared by the swirling flow method using a commercial NB generator had a mean particle size of 185 ± 57 nm (standard deviation) and a particle density of 7.0×10^7 mL^{-1}. We used aerated tap water as control water, and the initial dissolved oxygen (DO) concentration in surface water was comparable to that equilibrated with ambient air at a given temperature (Fig. 2). On the other hand, the initial DO in oxygen NB water a few hours after the preparation was still 1.5 times that in control water and the DO remained higher within 24 hours. Under different soil conditions in labile carbon content (i.e., high in experiment 1, middle in 2, and low in 3), the total CH_4 emission dissolved into leaching water for 56 days was 20%–28% lower in oxygen NB water than in control water (Fig. 3). Measuring DO profile at 1-mm intervals at the soil–water interface using an oxygen microelectrode and a micromanipulator, we found that oxygen depletion at shallow depths (4–15 mm from the soil surface) was ameliorated by oxygen NB water on day 35 of experiment 2 (Fig. 4). The result confirms that irrigation with oxygen NB water reduces CH_4 production in a flooded paddy soil through oxygenation of shallow soil.

The results provide researchers with the scientific basis for the use of oxygen NB water as a measure to control redox conditions in various aquatic environments, including flooded paddy soils. There is still room for improvement in soil oxygenation by raising the irrigation frequency. Further study is necessary to elucidate whether the oxygen is in dissolved form and/or as intact particles when delivered to a flooded soil through oxygen NB water.

(K. Minamikawa, T. Makino [Tohoku University, Japan])

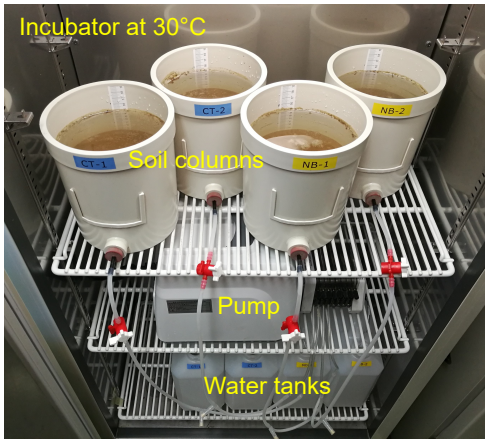

Fig. 1. Apparatus consisting of soil column systems for the three experiments

Water is leached at a fixed rate (1.73 cm day^{-1}) by the pump.

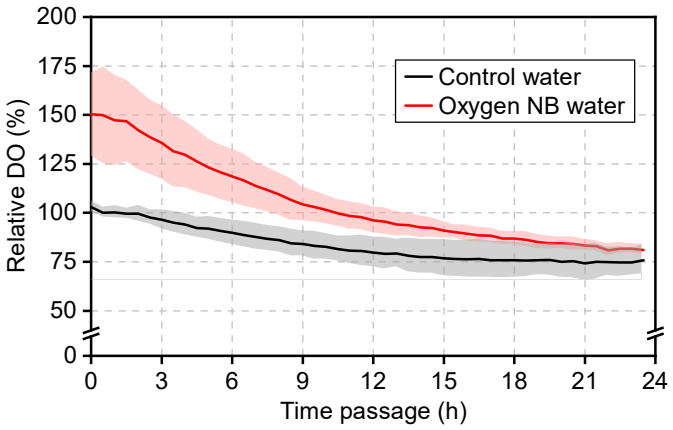

Fig. 2. Temporal shifts in surface water DO in Experiment 2

Values relative to that equilibrated with ambient air at a given temperature.

Solid lines indicate the means of four measurements, and bands indicate the standard deviations.

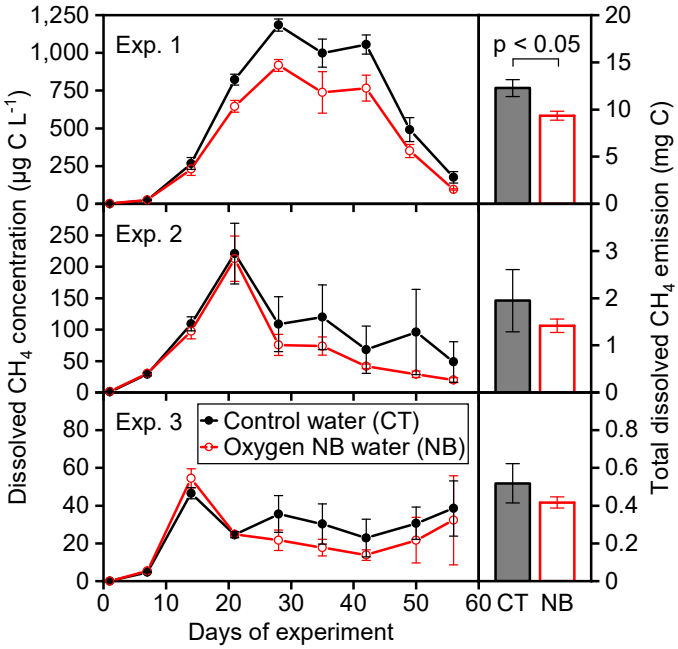

Fig. 3. Temporal shifts in dissolved CH_4 concentrations (left panels) and the total emissions (right panels) in the three experiments

Vertical bars indicate the standard errors (n = 3).

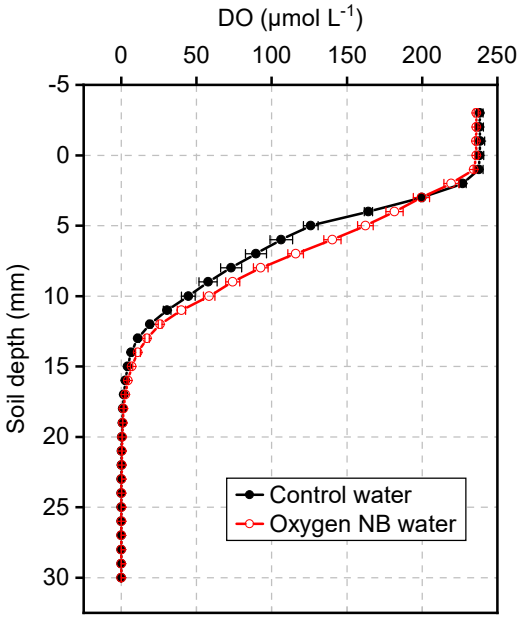

Fig. 4. DO profiles at the soil–water interface on day 35 of Experiment 2

Horizontal bars indicate the standard errors (n = 3).

Farmland reclamation using micro-dam sediments in the Ethiopian Highlands

The Ethiopian Highlands in the eastern part of sub-Saharan Africa typically experience semi-arid climatic conditions, with rainfall during rainy seasons causing severe soil erosion. Ninety-two (92) micro-dams have been constructed at micro-watersheds in Tigray, Ethiopia, more than half of which undergo sedimentation due to gully erosion, consequently decreasing the amount of available water. Sediment accumulation in micro-dams is considered a serious problem affecting irrigation water supply and crop cultivation (Berhane et al., 2016). Although it is an urgent challenge to remove the sediments from micro-dams, it is difficult to deal with, thus the problem remains unsolved. The purposes of this research are to estimate the storage water and sediment volume in a typical micro-dam at a micro-watershed in this region and to test the feasibility of using the sediments for farmland reclamation.

The Adizaboy micro-dam is located at the outlet of the steep Adizaboy micro-watershed (8.5 km^2). Weather conditions and water depths in Adizaboy micro-dam were automatically recorded. The storage volume change was assumed to be zero (0) for one year. Potential available water was calculated using the water balance analysis of Adizaboy micro-dam (Fig. 1). A new bathymetric survey method was applied to estimate the sediment volume in the micro-dam. The geographic coordinates along the water surface perimeters and the storage water depths were noted (Fig. 2, top). Sediment volume between observed sediment surface and estimated bottom surface was calculated (Fig. 2, bottom). Bare lands were cleared at the end of dry season (an agricultural off-season), when there was no storage water in the micro-dam. Sediments were excavated manually and transported using farm animals. A farmland was reclaimed by forming layers of stones and sediments (Fig. 3).

The reclaimed farmland will be managed by Wareda (the villagers' group) and provided for free to some young landless farmers to create employment opportunities. By cultivating vegetables with high market value, the reclaimed farmland is expected to generate a cash income source and improve the living standard of residents. Onion yield in the reclaimed farmland of 11.93 t/ha is almost same as the national average (10.38 t/ha). It is thus necessary to construct a farm pond for irrigation to enable vegetable cultivation during the dry season. To extend the technology, it would be practical to use past experiences and knowledge of participants in cooperation with local governments, universities, and residents in the selection of sites, earth works, and construction of additional facilities etc. This method of estimating the volume of sediments is applicable to other micro-dams.

(K. Koda, G. Girmay [Mekelle University], T. Berihu [Mekelle University])

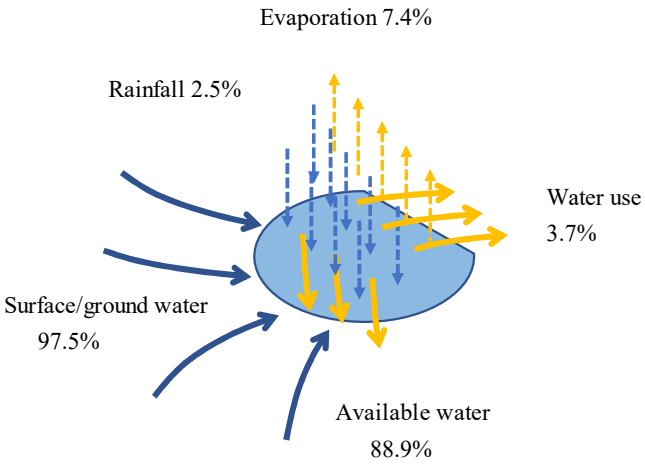

Fig. 1. Water balance of Adizaboy micro-dam

The storage volume of the micro-dam is 200,000m^3. Available water is assumed to be the sum of water leakage through the foundation rock and the embankment, the flood water over the spillway, and the spring water downstream.

Fig. 3. The reclaimed farmland using sediments from Adizaboy micro-dam

Top: before reclamation, Bottom: after reclamation

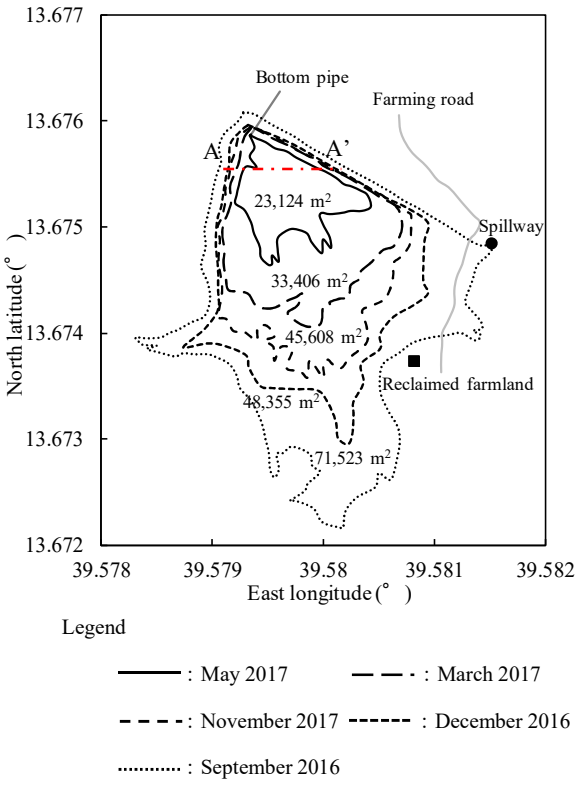

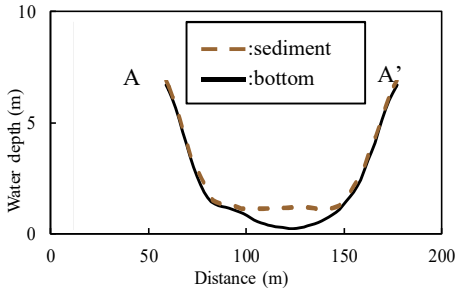

Fig. 2. Changes in water storage area and cross-sectional view of Adizaboy micro-dam

Top: changes in water storage area, Bottom: cross sectional view

The numbers in the top figure show the water storage areas (in m^2). The water depth in the bottom figure displays the height from the lower edge of the bottom pipe inlet. The sediment volume of Adizaboy micro-dam is estimated to be 6,400 m^3. In case the thickness of the reclaimed farmland is 0.2 m, the reclaimable farmland area is 3.2 ha. It would also be effective if some of the sediments are removed and used for reclamation before the bottom pipe gets buried and malfunctions.

Assessing nanoparticulate lime and phosphate rock and increasing their efficiency as a liming agent and phosphorus source, respectively

Acid soils occupy approximately 43% of the world's tropical land area. Although they have high potential for agriculture production, plant growth is hindered by the low availability of P, Ca, and Mg, and the acidity-related toxicity of Al, Fe, and Mn. Application of conventional lime and soluble P fertilizer is considered general practice for correcting acidity and nutrient deficiencies in acid tropical soils. As the prices of lime and P fertilizers have increased markedly worldwide, there is an urgent need for new materials that achieve goals at a reduced cost.

Nanoparticulate lime (NL) or phosphate rock (NPR) can be used as an alternative by increasing its efficiency. Reducing the particle to nanoscale (Fig. 1) and thus increasing the total surface area could offer a mechanism to increase the efficiency of lime and phosphate rock (Devnita et al. 2018, Liu and Lal 2015). This study was, therefore, conducted to assess NL and NPR to increase their efficiency as a liming agent and phosphorus source, respectively.

Applying NL to the top 5 cm at 40 and 80 kg ha^{-1} was effective at increasing the downward movement of Ca and the neutralization of soil acidity (in terms of pH) to 20 cm depth, as well as rectifying Al toxicity (in terms of exchangeable Al) to ≤ the critical limit to 10 cm (Fig. 2). The NL at 80 kg ha^{-1} was most economically justified in terms of rectifying Al toxicity throughout the profile.

NPR (Fig. 1) significantly affected soil pH after harvest (Fig. 3). NPR at 250 kg ha^{-1} and 500 kg ha^{-1} increased soil pH, though not to the levels required to promote spinach growth, while NPR at 1,000 and 2,000 kg ha^{-1} increased soil pH within the optimum range (typically 6.4-6.8). Increasing NPR significantly increased available P after harvest. NPR at 2,000 kg ha^{-1} released 56 mg P kg^{-1} (upper limit for spinach), while NPR at 1,000 kg ha^{-1} released 35 kg P ha^{-1} (target limit).

NPR significantly increased dry matter yield (DMY, Fig. 4). NPR at ≥1,000 kg ha^{-1} increased DMY by ≤11.5x the initial value, while NPR at <1,000 kg ha^{-1} increased DMY by ≤3x. DMY did not increase significantly from 1,000 to 2000 kg ha^{-1}. Therefore, the critical threshold or application rate that produced the maximum yield (2.3 g DMY $plant^{-1}$) is 1,000 kg ha^{-1}. NPR also significantly increased leaf P. NPR at 2,000 kg ha^{-1} increased leaf P the most, but not significantly more than at 1,000 kg ha^{-1}. The leaf P concentration varied from 0.1% to 0.53% among NPR rates. When NPR rate was ≥1,000 kg ha^{-1}, leaf P was about ≤5.8x the initial value. According to the diagnostic range for P in spinach leaf, NPR at ≥1,000 kg ha^{-1} increased available soil P to at least the upper limit.

In summary, the soil and plant parameters increased to the same degree at 1,000 and 2,000 kg ha^{-1}. Therefore, the use of 1,000 kg ha^{-1} is more economically justified. Regular application of NPR and further research for economic comparison between NPR and both of lime and superphosphate will be needed.

(H. Omae, A. A. Abd-El Halim [Tanta University])

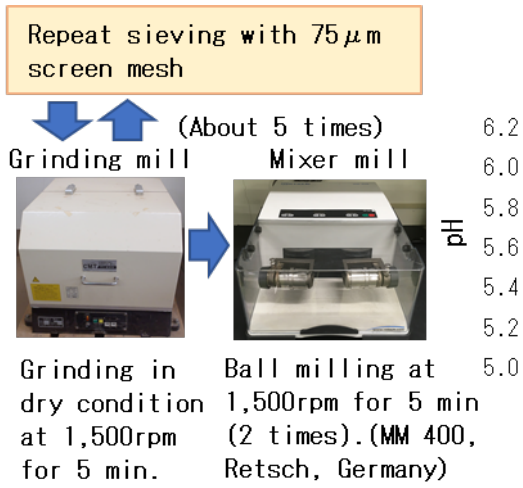

Fig. 1. Nanoparticulation process

Burkina Faso phosphate rock was used.

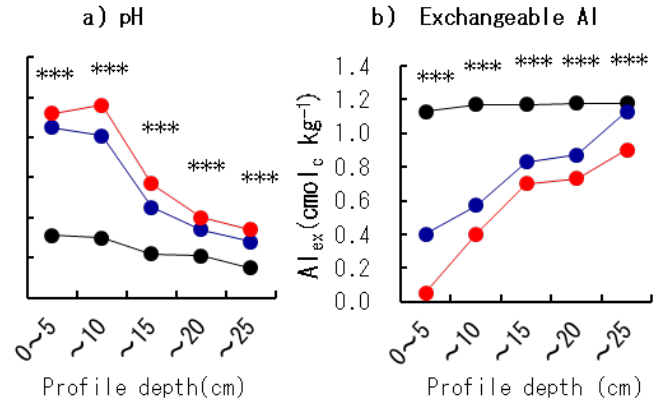

Fig. 2. pH and exchangeable Al of the simulated plough layer with a different nanoparticulate lime (NL)

NL leached with 28cm of water over 40 days; ***: p<0.001 (ANOVA)

0 kg ha^{-1} 8 kg ha^{-1} 80 kg ha^{-1}

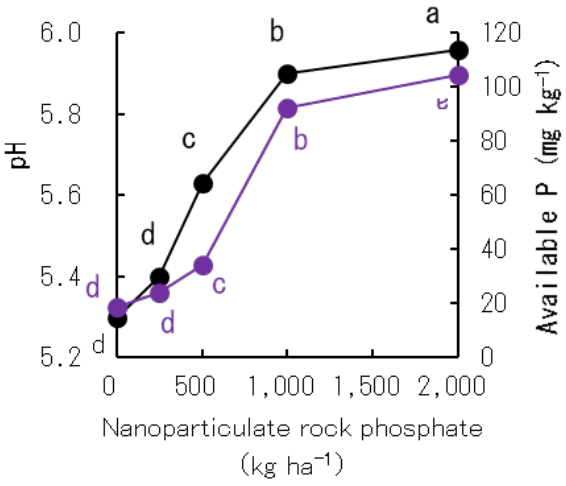

Fig. 3. Effects of nanoparticulate phosphate

Data were collected at the end of the growth period (49 days) after pre-incubation (21 days). Different letters show significant difference (Tukey's HSD).

pH Available P

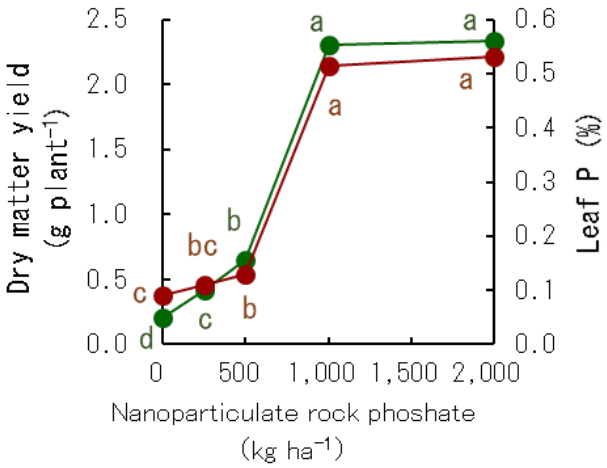

Fig. 4. Effects of nanoparticulate phosphate rock on spinach dry matter yield and leaf P concentration

Data were collected at the end of the growth period (49 days) after pre-incubation (21 days). Different letters show significant difference (Tukey's HSD).

Dry matter yield Leaf P

Biological nitrification inhibition of sorghum is related to the inhibition of ammonia-oxidizing archaea

To increase crop production, farmers often apply high amounts of nitrogen fertilizers in agricultural lands. The resulting high nitrification activity greatly contributes to global warming due to the release of the potent nitrous oxide (N_2O) gas. Furthermore, this practice not only causes environmental water pollution due to leakage of nitrate nitrogen, but also lower use efficiency of the fertilizer nitrogen and reduced crop yields. Biological nitrification inhibition (BNI), a crop-mediated complex molecular mechanism in which the crop suppresses soil nitrification by itself, is gaining much attention as a suitable technique to mitigate the above problems. Here we look at sorghum, the world's fifth-ranked cereal in terms of production area. Sorghum secretes sorgoleone, a compound that has shown BNI ability, from its roots.

In this study, we clarified the relationships between the amount and the location of sorgoleone secretion from the plant's roots, and the rhizosphere soil microbial communities through a pipe cultivation test (Fig. 1). 296B shows the least sorgoleone secretion, followed by IS32234 then IS20205 (Fig. 2). The secretion increases towards deeper layers at the newer root zone. The application of 120 kg ha^{-1} nitrogen as ammonium sulfate solution to the topsoil, greatly enhances the nitrification activity in the 0-10 cm soil layer, which remained low in the deeper layers (Fig. 3). In the 0-10 cm soil layer, 296B showed the highest nitrification activity, followed by IS32234 and IS20205, which opposes with the sorgoleone secretion. These results indicate that sorgoleone plays a substantial role in sorghum's ability to exert BNI. The number of ammonia-oxidizing bacteria (AOB) and archaea (AOA) in the 0-10 cm soil layer was determined by qPCR, targeting the ammonia monooxygenase (*amoA*) gene. The number of AOA was inversely related to the amount of sorgoleone and was proportional to the nitrification activity. However, we observed no change in the number of AOB (Fig. 4). This shows that the nitrification in sorghum rhizosphere soil is related to the effect of sorgoleone secreted from the roots of sorghum, which suppresses AOA among the microorganisms harboring the *amoA* gene. The study also shows the contribution of other factors, such as soil pH, water content, organic and inorganic nitrogen content, to the ability of sorghum to exert BNI.

These findings demonstrate the great influence of the suppression of AOA on sorghum BNI. In addition, the ease of handling of root and soil samples by soil depth, makes this pipe cultivation test useful for BNI research of other plants.

(P.S. Sarr, Y. Ando, S. Nakamura, G.V. Subbarao,
S. Deshpande [International Crops Research Institute for the Semi-Arid Tropics])

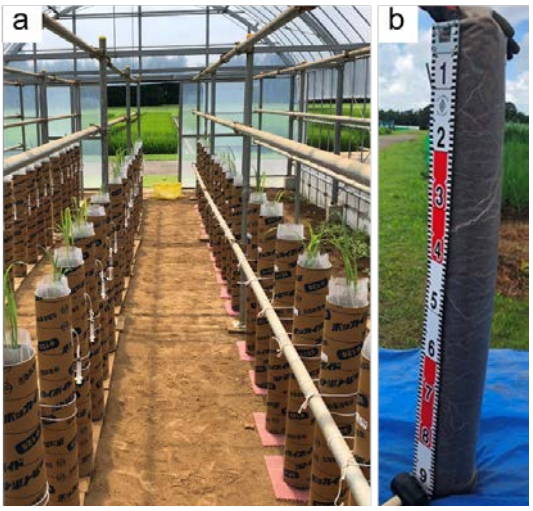

Fig. 1. Sorghum pipe (12 cm x 1 m) cultivation test in greenhouse at 31 days after seeding (a), and soil column removed from pipe at the first soil and plant root sampling (b)

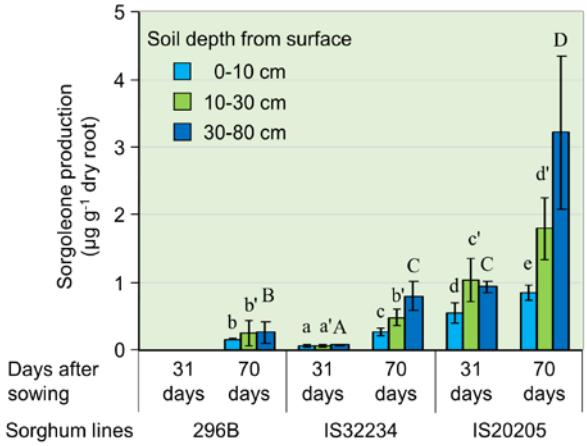

Fig. 2. Dynamics of sorgoleone secretion from roots of sorghum along the soil profile under nitrogen fertilizer application (120 kg ha^{-1})

Bars in the figure indicate standard deviations. The same type of letter (x, x′, X) compares the differences of sorgoleone secretion between sorghum lines by soil depth, and values with the same letter are not significantly different at p<0.05.

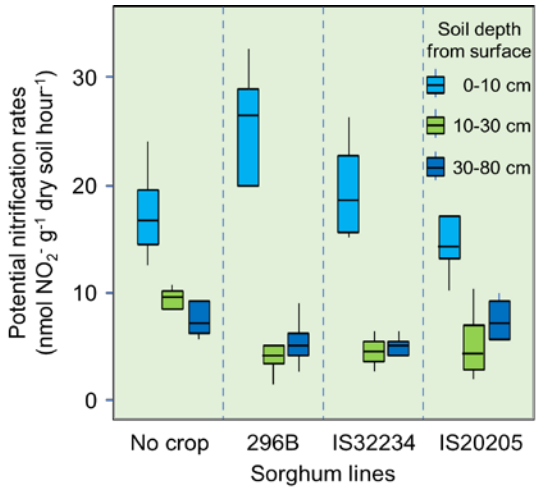

Fig. 3. Nitrification activity in bulk (no crop) and sorghum rhizosphere soils along the soil profile at 70 days after seeding, under nitrogen fertilizer application (120 kg ha^{-1})

The boxes in the figure indicate the interquartile range, and the bars indicate the maximum and minimum values. Soil layers below 10 cm depth have less ammonium applied, so their nitrification activity does not increase and the effect of sorgoleone does not appear.

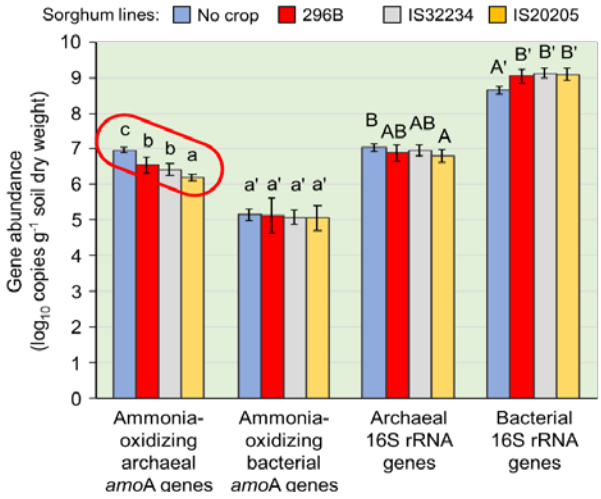

Fig. 4. Gene abundance in bulk (no crop) and rhizosphere soils (0-10 cm layer) of sorghum lines cultivated for 70 days under nitrogen fertilizer application (120 kg ha^{-1})

amoA: Ammonia monooxygenase α subunit gene. Bars in the figure indicate standard deviations. The same type of letter (x, x′, X, X′) compares the differences of the abundance of each gene, and values with the same letter are not significantly different at p<0.05. The gene abundance below 10 cm showed a similar trend.

Solubility improvement of African low-grade phosphate rock through calcination with potassium carbonate

Although many phosphate deposits have been found in sub-Saharan Africa, farmers are facing high prices of P fertilizers because of the low solubility of the African low-grade phosphate rocks (PRs). We have previously reported that PR calcination with Na carbonate improves the solubility of these PRs, but their application showed limited crop growth, especially in upland conditions. It was speculated that Na accumulation in the soil caused plant growth inhibition. Therefore, we tried to elucidate the effect of calcination with potassium carbonate (K_2CO_3) on PR solubility and its application effects for lowland rice and maize through pot experiments.

We used Kodjari PR produced in Burkina Faso for the calcination. Fine powdered PRs were mixed with K_2CO_3 in five doses to achieve the target K_2O compositions of 200, 250, 300, 350, and 400 g kg^{-1}. The mixtures were pressed with distilled water to form coin-shaped pellets. Then, the pelletized PR-K_2CO_3 mixtures were calcined at 900, 1000, 1050, and 1100 °C for 10 min using a muffle furnace. The pot experiments were conducted for 56 days, monitoring the growth of rice and maize under several application rates.

As a result, the solubility reached about 100% in 20 g L^{-1} citric acid and about 40% in water. This shows that K carbonates behave like Na carbonate in the solubilization of low-grade PRs in Burkina Faso. The calcinated Burkina PR (CB) application in the application rates up to 1 g P_2O_5 pot^{-1} yielded comparable plant growth to that of triple super phosphate (TP). K carbonate calcination deterred Na accumulation in the soil, and it was effective for soil P fertility improvement and plant growth. The calcination technology can be conducted by external heating U-turn rotary kiln using solar power.

(S. Nakamura, F. Nagumo, T. Kanda, T. Imai [Taiheiyo Cement Corp.],
J. Sawadogo [INERA])

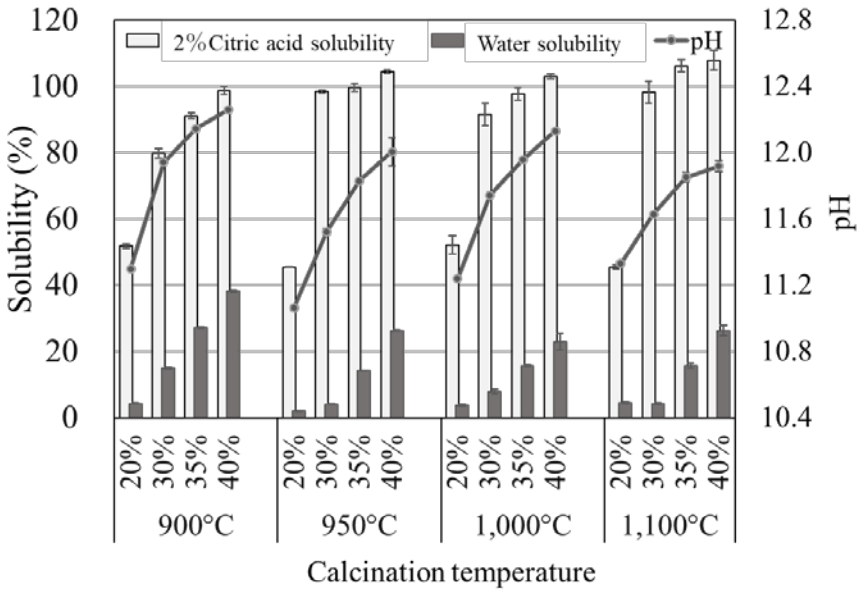

Fig. 1. Solubility changes of Burkina Faso phosphate rock through calcination with several compounding rates of potassium carbonate under four levels of temperature
Error bars are standard errors (n =3)

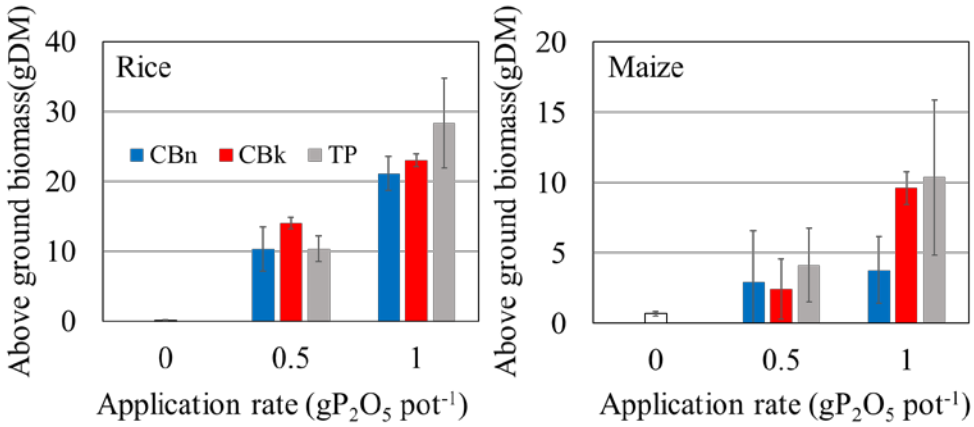

Fig. 2. Application effects of phosphate rocks calcinated with Na carbonate and K carbonate on rice and maize

Error bars are 95% confidence intervals (n=3). CBn: Calcinated PR with Na carbonate, CBk: Calcinated PR with K carbonate, TP: Triple super phosphate

Table 1. Soil chemical properties after several phosphate fertilizer applications

Crop/Soil water condition	Fertilizer	pH		EC		Available P				Exchangeable cation							
						Bray I		Bray II		Ca		Mg		K		Na	
				mS m^{-1}		mgP kg^{-1}				cmolc kg^{-1}							
Rice/ Submerged	None	5.84	c	108	c	0.08	b	6.39	d	3.31	c	0.70	bc	0.28	b	0.15	c
	BP	5.72	c	110	c	0.16	b	107	c	3.18	c	0.64	c	0.24	b	0.16	c
	CBk	6.45	a	183	a	6.34	a	141	a	10.2	a	0.78	b	6.67	a	0.28	a
	TP	6.10	b	141	b	4.94	a	117	b	5.42	b	1.09	a	0.47	b	0.24	b
Maize/ Upland	None	5.85	a	114	b	0.09	b	6.77	c	3.39	c	0.69	b	0.3	b	0.14	c
	BP	5.70	a	123	b	0.17	b	96.1	b	3.56	c	0.69	b	0.33	b	0.15	c
	CBk	5.97	a	189	a	5.81	a	158	a	9.36	a	0.73	b	6.39	a	0.21	b
	TP	6.28	a	168	a	5.69	a	107	b	5.90	b	1.11	a	0.49	b	0.24	a

None: No P application, BP: Burkina Faso PR, CBk: Calcinated PR with K carbonate, TP: Triple super phosphate. Bray I, and Bray II are available P content determined by Bray I method and Bray II method, respectively. Alphabet difference indicates significant differences (p<0.05) by Tukey HSD method.

Fig. 3. External heating U-turn rotary kiln for calcination (Burkina Faso, INERA-Kamboinse)

Soil phosphorus availability for rice plants can be rapidly estimated by laboratory visible and near-infrared spectroscopy

Phosphorus (P) deficiency is a major constraint to rice production in highly weathered soils of tropical agroecosystems. Therefore, rapid evaluation of soil phosphorus availability is crucial toward realizing efficient fertilizer management for increasing crop production. As a laboratory proximal sensing technique, the capability of visible and near-infrared (Vis-NIR) spectroscopy with partial least squares (PLS) regression to determine soil properties has been demonstrated. However, the evaluation of soil P is still a challenging task. Thus, we aimed to develop a model for estimating oxalate-extractable P (Pox), which represents the soil P supply capacity for rice crops in lowland and upland fields in the central highlands of Madagascar.

Pox content was measured for soil samples (n = 51) collected from the surface layer (0–15 cm depth) in rice fields in the central highlands of Madagascar. Large spatial variations in Pox were observed in soil samples collected from a wide range of soil types over a wide area and even in soil samples from a village (Fig. 1). This highlighted the importance of developing a prompt assessment method for P availability in multiple soil samples. Soil samples were scanned by a portable spectroradiometer (FieldSpec, ASD Inc.) in a dark room to measure spectral reflectance in the Vis-NIR region (400–2400 nm), and subsequently a calibration model was developed for estimating Pox using selected wavebands on first derivative reflectance spectra with genetic algorithm-based PLS regression (GA-PLS). With this PLS model, Pox content in soil can be rapidly estimated with high accuracy and reproducibility (Fig. 2). The selected wavebands in the GA-PLS model were found to be relevant to chemical associations of Pox in soils bound to Al and Fe oxides and organic compounds (Fig. 3).

The Pox content can be accurately and rapidly predicted from laboratory Vis-NIR spectroscopy with GA-PLS regression; it takes only one minute to measure the spectral reflectance for one soil sample. Therefore, the calibration model can be applied to assess the P deficiency level with high spatial variation in lowland and upland rice fields for appropriate fertilizer management. Research institutes, such as regional agricultural research centers or universities, can help handle the measurement because the portable spectroradiometer is not affordable for local farmers. An alternative cheap edition of the spectroradiometer using specific wavebands relevant to soil chemical associations of Pox in soils is needed. Further applicability of this model should be tested particularly in soils with high pH and Ca-associated P content, and in soils with high sand content.

(T. Nishigaki, K. Kawamura, Y. Tsujimoto, A. Andriamananjara, M. Rabenarivo, T. Rakotoson, T. Razafimbelo [Antananarivo University])

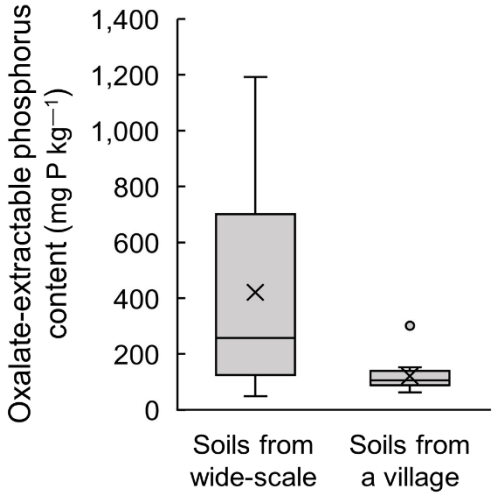

Fig. 1. Spatial variation of oxalate-extractable P

The bar on the left indicates Pox content of soil samples collected within an area of 100 km radius (n = 35), and the bar on the right indicates Pox content of soil samples collected within a village (n = 16). The coefficients of variance are 0.85 and 0.45, respectively.

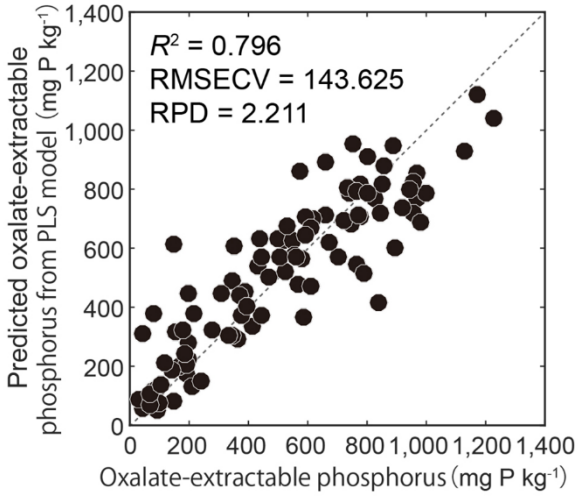

Fig. 2. Relationship between observed and predicted values of soil oxalate-extractable P using the PLS model

RMSECV: Root mean squared errors of cross-validation using the leave-one-out method.

RPD: Residual predictive deviation. The criteria for determination are (1) RPD < 1.15: unpredictable, (2) 1.16–1.40: weakly correlated, (3) 1.41–1.70: screening with low accuracy, (4) 1.71–2.42: capable of screening, and (5) >2.43: possible to estimate with practical accuracy.

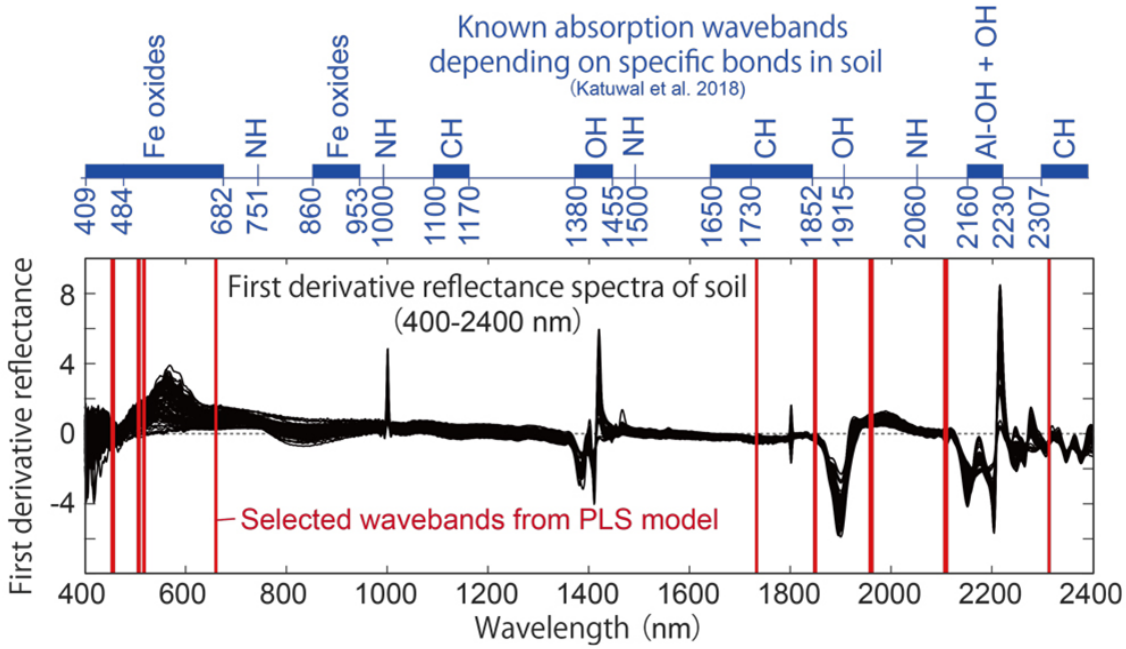

Fig. 3. Selected wavebands (red bars) in the PLS model

A new indicator of leaf stomatal conductance based on thermal imaging

Stomatal conductance is a major regulator of water vapor and carbon dioxide exchange between the leaf and the surrounding air, directly affecting plant growth and leaf water status. To rapidly evaluate the stomatal conductance, indicators from infrared thermal imaging are available as an easy and simple method. However, a difficulty with these indicators is that the relationship between leaf temperature and stomatal conductance may vary strongly with variations in solar radiation, air temperature, humidity, and wind speed, and thus it is difficult to estimate stomatal conductance from leaf temperature over a wide range of different meteorological conditions.

In this study, a new indicator of stomatal conductance (GsI) with environmental robustness was developed. This indicator is calculated from leaf temperature and other meteorological variables of solar radiation, air temperature, and relative humidity (Fig. 1). The equation is the result of a modification of the theoretical equation of stomatal conductance, simplified by making several assumptions. To validate the robustness of the GsI under varied meteorological conditions, thermal image was obtained for cowpea plants every week from two to eight weeks after sowing. Four cowpea varieties were grown at the experimental field of the International Institute of Tropical Agriculture (IITA) in 2016 and 2017. Compared to the existing indicator of stomatal conductance (air-leaf temperature difference), the GsI showed stable relationship with measured stomatal conductance using leaf porometer over the different meteorological conditions (Fig. 2).

GsI was calculated using a simplified equation with four variables, namely, leaf temperature, air temperature, relative humidity, and solar radiation. Except for leaf temperature, all other variables can be obtained from continuous-measurement devices installed near the field; thus, an evaluator only needs to take a thermal image for each measurement. As GsI calculation does not require any reference temperature, the time for photographing is much shorter than that for evaluations with reference temperatures. Therefore, this new method is suitable for rapidly evaluating a large plant population, such as a set of genetic resources and cross-populations, for genetic analysis.

Although the relationship between GsI and measured stomatal conductance is stable for varied meteorological conditions, there are precautions for its application. First, the GsI is not suitable for plant leaves with different angles because the relationship between thermal image and actual temperature differs depending on the leaf angle. Second, GsI should not be applied to leaves having extremely low stomatal conductance such as under severe drought conditions or deeply clouded conditions. This is because the equation of GsI is premised on the occurrence of transpiration at leaf surface. Determination of stomatal conductance using GsI with the above precautions provides important physiological information related to plant responses to the environment, and will help identify superior genotypes with high adaptability to specific target environments.

(K. Iseki, O. Olaleye [International Institute of Tropical Agriculture])

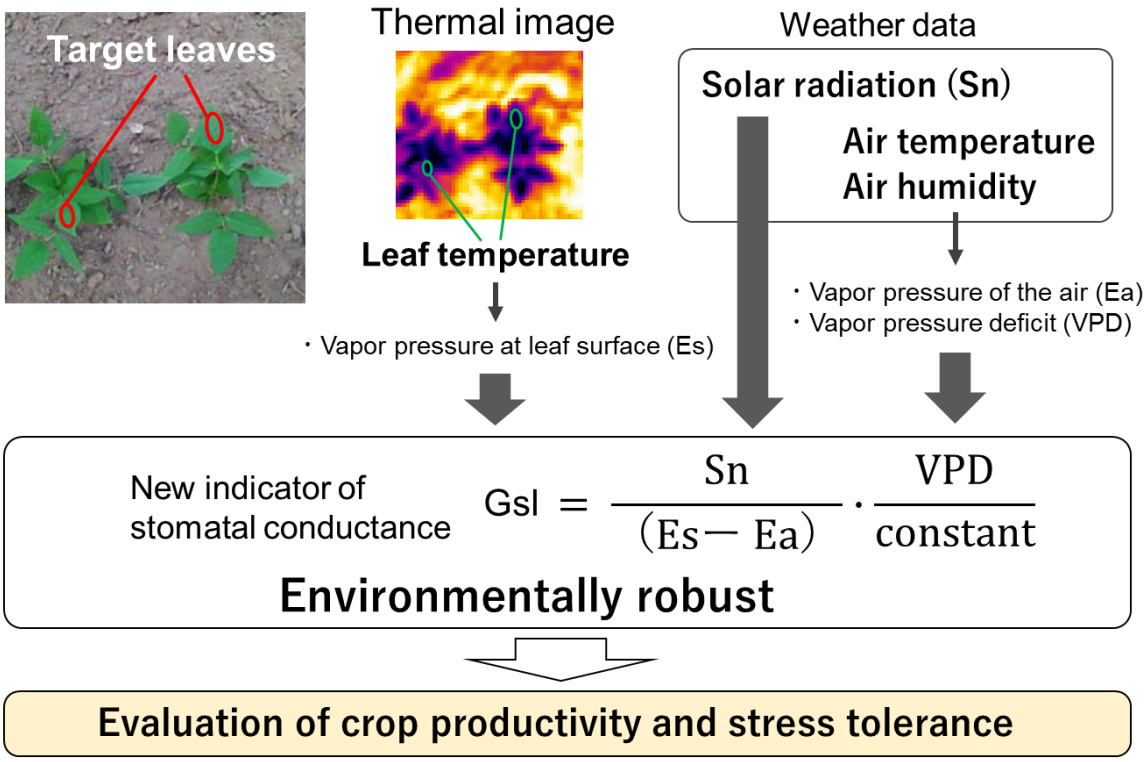

Fig. 1. A new indicator of stomatal conductance (GsI)

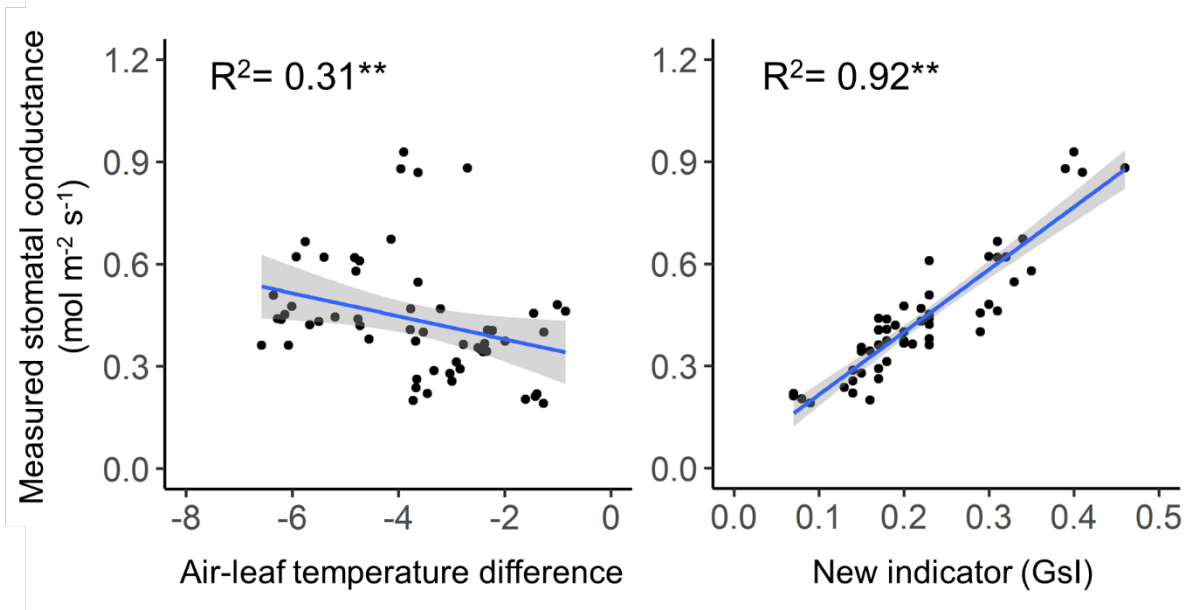

Fig. 2. Relationships between indicators based on thermal imaging and measured stomatal conductance. Gray area represents 95% confidence interval of the regression line.

SSR marker technology package for variety identification of white Guinea Yam

White Guinea yam (*Dioscorea rotundata*), one of the most important cash crop for farmers and a major staple food for the people of West Africa, retains huge potential for alleviating widespread poverty and hunger in the region. Now, yam research is at a turning point, and recent advancements in genetics and mass propagation are expected to boost breeding efficiency and dissemination of improved varieties. On the other hand, since it is difficult to distinguish varieties based on the visible characteristics of the shoot and tuber of yam (Fig. 1), mechanical mixture between varieties grown in the same field has been a serious problem through all the steps in the breeding and propagation process, including planting, cultivation, harvesting, and storage. To overcome this problem, a simple tool to identify varieties was highly desired.

To enable variety identification of white Guinea yam, a Simple Sequence Repeat (SSR) marker system was adopted based on its various advantages such as high reproducibility, low cost, and high polymorphism. In the initial setup, 16 SSR markers that can be used to distinguish varieties and genetic resources effectively were selected from the 90 SSR markers developed in our previous study (JIRCAS Research Highlights 2015, B05) (Fig. 2). Additionally, various tools to enable successful variety identification using the developed SSR markers and maximize the benefits to users in the breeding and seed sectors were subsequently developed. For example, the developed web application “Minimum SSR Marker Finder for Guinea yam” (https://www.jircas.go.jp/en/database/yam_toolkit/finder) linked with the database contains SSR polymorphism data of over 550 varieties and lines (as of February 2020), and supports identification of the minimum set of SSR markers that can distinguish the varieties selected by each user. In addition to the conventional DNA extraction method using a young leaf sample, we developed the “Sample collection and DNA extraction methods for tuber skin” to widen the user’s choice of period to conduct variety identification (Fig. 3). Also, the proposed “Sample bulking method” specially designed for large-scale propagation of yam seed tubers, enables the yam seed sector to reduce time and cost in quality control and quality assurance (Fig. 4).

These useful tools and methods were assembled as an “SSR marker technology package for variety identification of white Guinea yam” to cover all necessary steps to distinguish varieties (Fig. 5), and the website titled “Yam variety identification toolkit” (https://www.jircas.go.jp/en/database/yam_toolkit) was launched to support users in conducting variety identification with various guidance, tips, manuals, videos, and images. The technology package can reduce time and cost, and provide flexibility for users to ensure the uniformity of the materials before planting, prevent mechanical mixture in various stages of cultivation, and assure the quality of the products. We expect this technology package to support seed growers, extension officers and inspection officers, as well as yam researchers involved in various stages of yam improvement and dissemination. This in turn could help boost breeding efficiency and dissemination of improved varieties, and further improve food security and livelihood in West Africa.

(S. Muranaka, S.Yamanaka, M.Tamiru [Iwate Biotechnology Research Center],
P. Agre [International Institute of Tropical Agriculture])

Fig. 1. White Guinea yam (*D.rotundata*)
Left: Shoots of multiple varieties grown in a farmer's field
Right: Tubers obtained from a single plant (DrDRS-139)

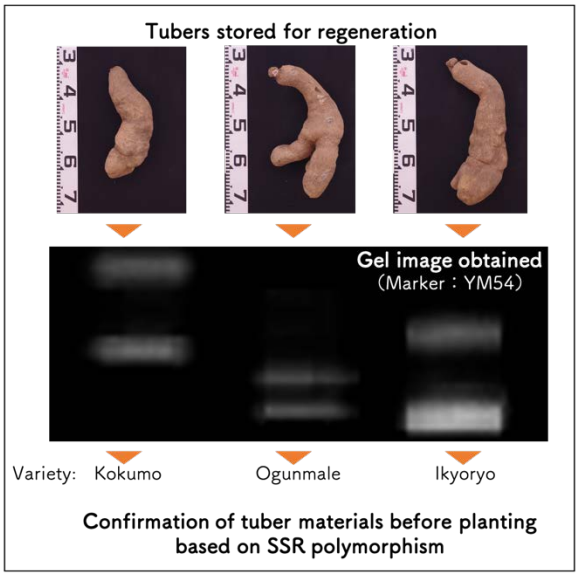

Fig. 2. Identification of varieties with similar tuber shapes using SSR markers

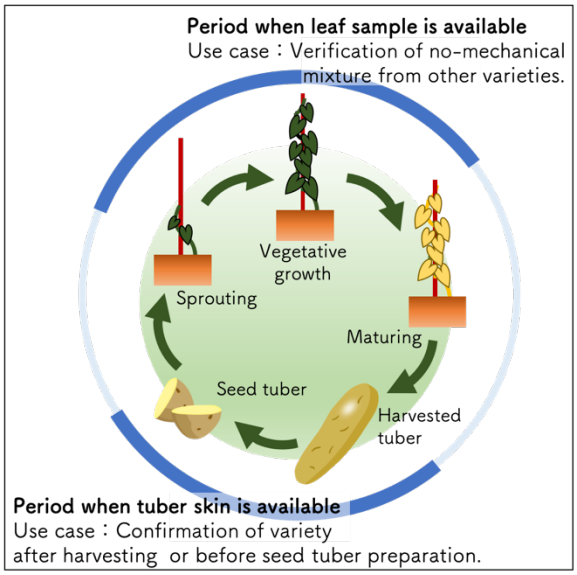

Fig. 3. Expanded period for variety identification with two types of samples

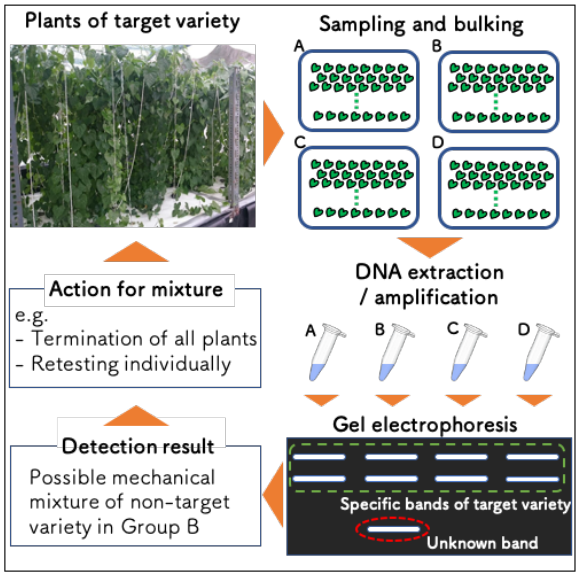

Fig. 4. Utilization of the sample bulking method to maintain purity of target variety

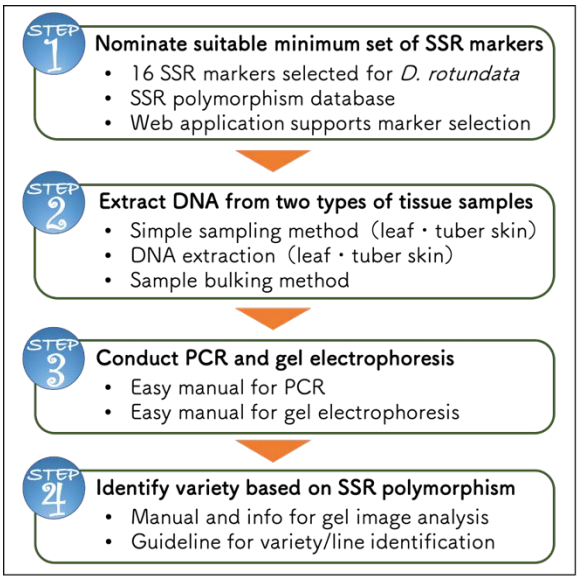

Fig. 5. SSR marker technology package for variety identification of white Guinea yam

SPIKE, a quantitative trait locus for increasing the number of spikelets per panicle, enhances rice grain yield under low-yield conditions

Rice is an important food source in Asia and Africa; however, poor soil fertility and nutrient availability considerably limit rice production in these regions. In addition, the majority of local farmers lack the finances to purchase sufficient fertilizer. Therefore, it is necessary to develop genetically improved rice varieties with high nutrient-use efficiencies. Previously, a quantitative trait locus, *SPIKE*, was reported to have increased the number of spikelets per panicle in rice. Because tillering, and thus the number of panicles, is restricted under nutrient-poor soils, we expected that *SPIKE* may be useful in enhancing rice productivity under low-yield conditions.

In this study, we grew IR64 and the near-isogenic line (NIL) for *SPIKE* in the IR64 genetic background. They were grown in research plots at the International Rice Research Institute (IRRI) in the tropics across 11 seasons from 2011 to 2017, and in 2018 under high and low nitrogen (N) fertilizer conditions, where mean yield variation was 4.2–6.7 t ha^{-1}. In multiseasonal trials, overall yield performance of NIL-*SPIKE* was 11% superior to that of IR64. Significant variety × season interaction clarified that NIL-*SPIKE* was superior to IR64 in the lower-yield seasons (< 5 t ha^{-1}) but the difference decreased or disappeared completely in the higher-yield seasons (> 5 t ha^{-1}) (Fig. 1). A subsequent N application trial with two levels of N fertilizer (45 and 180 kg N ha^{-1}) confirmed a similar variety × N interaction for *SPIKE*; NIL-*SPIKE* tended to be superior to IR64 for grain yield under low-N application (4.3 t ha^{-1}), while the difference disappeared under high-N application (6.75 t ha^{-1}) (Fig. 2). The advantage of NIL-*SPIKE* under low-N application was due to more spikelets m^{-2} compared to IR64 but the difference disappeared under high-N application because there were fewer panicles m^{-2} in NIL-*SPIKE* compared to IR64 (Fig. 3).

The results of this study indicate that *SPIKE* is effective at increasing rice yield under low-yield conditions (< 5 t ha^{-1}), namely low-N application or low soil fertility. Therefore, *SPIKE* should be used in breeding programs aimed at regions where soil fertility is poor, or where farmers cannot purchase adequate fertilizer.

(N. Takai, K. Sasaki, H. Asai, D. Fujita [Saga University], P. Lumanglas [IRRI], E.V. Simon [IRRI], T. Ishimaru [NARO], N. Kobayashi [NARO])

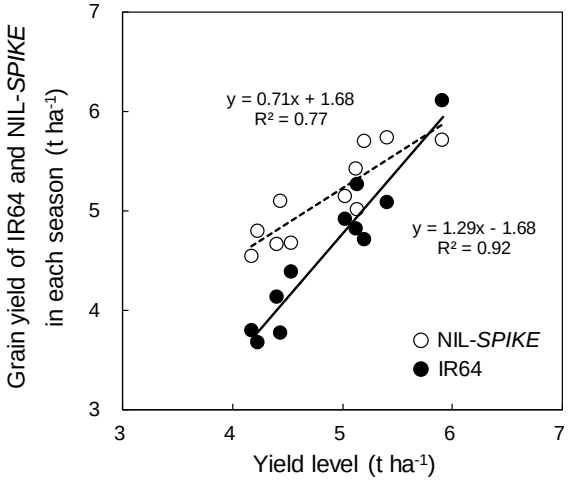

Fig. 1. Comparison of grain yield between IR64 and NIL-*SPIKE* across 11 seasons. Yield level shows mean yield between IR64 and NIL-*SPIKE* in each season.

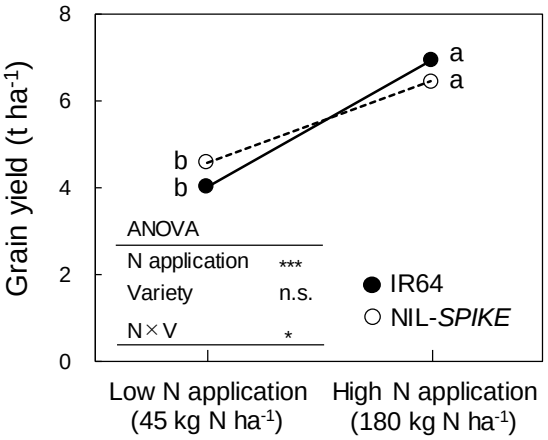

Fig. 2. Comparison of grain yield between IR64 and NIL-*SPIKE* under low- and high-N applications. *** and * show significance at 0.1% and 5% levels, respectively, while n.s. indicates not significant. Different letters show significant difference at 5% level.

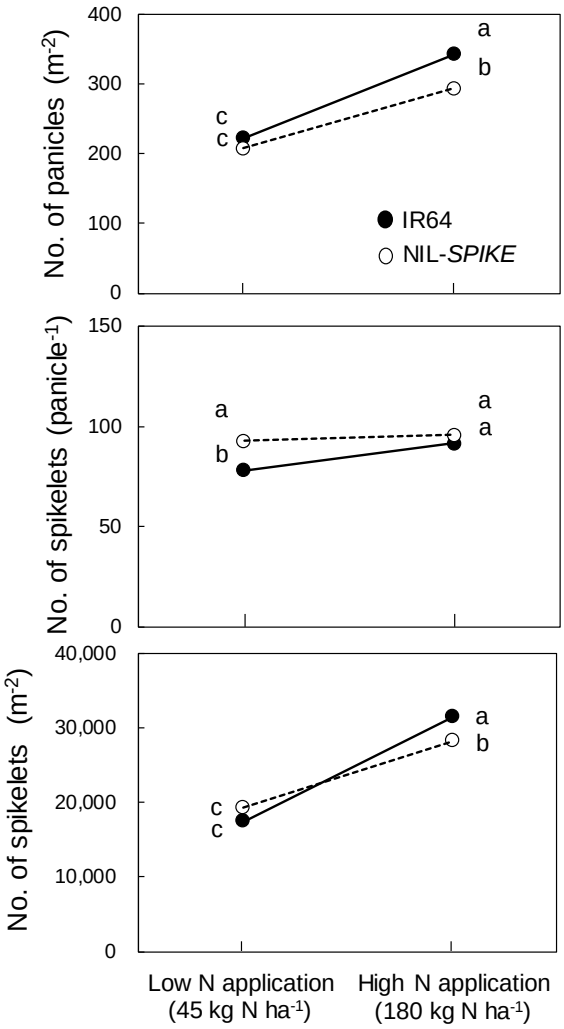

Fig. 3. Comparisons of the number of panicles m^{-2}, the number of spikelets per panicle, and the number of spikelets m^{-2} between IR64 and NIL-*SPIKE* under low- and high-N applications. Different letters show significant difference at 5% level.

Sugarcane and *Miscanthus* intergeneric hybrids: New sugarcane breeding materials with high photosynthetic activity in a low-temperature environment

Sugarcane (*Saccharum* spp. hybrid) is an essential crop for food and energy production in the world, hence improving its productivity is required. Sugarcane is one of several high-yielding crops with C_4 photosynthesis in tropical and sub-tropical areas; however, it is susceptible to low temperatures, and there are many production areas where low temperature is a major constraint in production. Therefore, improving its adaptability to low-temperature environments has been one of the important breeding targets in sugarcane. Among C_4 plants, *Miscanthus* spp., a sugarcane-related genus, is highly adapted to low-temperature environments because of its cold tolerance during photosynthetic activity, thereby receiving attention as a biomass crop in cold-climate regions. This study aimed to develop new sugarcane breeding materials for improving cold tolerance in sugarcane by intergeneric hybridization between sugarcane and *Miscanthus* spp.

Using intergeneric crosses between sugarcane clones KY06-139 and KY05-619 as female and Shiozuka (*Miscanthus sinensis*) and Miyakonojo (*M. Sacchariflorus*) as male, we developed two hybrids between sugarcane and Shiozuka and 16 hybrids between sugarcane and Miyakonojo (Fig. 1). In the chilling stress experiment (12–13°C day/7–9°C night), the *Miscanthus* parents and some hybrids exhibited higher photosynthetic rates than their sugarcane parents after 7 days and 14 days of chilling treatment (Fig. 1). Furthermore, in the post-chilling recovery experiment, where chilling treatment (12°C day/7°C night) was applied for 4 days and then recovery treatment (26°C day/18°C night) was applied for 7 days, the *Miscanthus* parents and some hybrids showed better recovery of photosynthetic rates than the sugarcane parents (Table 1). Intergeneric hybrid JM14-09 showed higher biomass productivity than sugarcane parent KR05-619 and *Miscanthus* parent Shiozuka, based on the results of field experiments in a cold-climate region (Fig. 2).

To sum up, the intergeneric hybrids developed in this study can be utilized as new breeding materials for improving the biomass productivity and photosynthetic characteristics of sugarcane at low-temperature environments.

(Y. Terajima, S. Ando, S. Kar [Hokkaido University],
T Yamada [Hokkaido University])

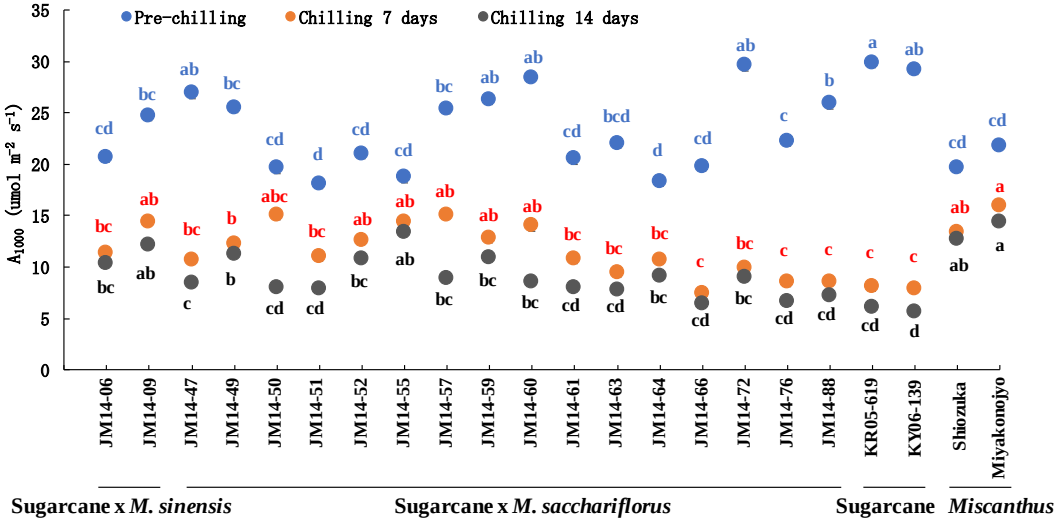

Fig. 1. Photosynthetic rates of intergeneric hybrids in the chilling treatment

The experimental materials were planted in plastic pots with three replications on October 28, 2016, and chilling treatment was started from December 22, 2016. Photosynthetic rates were measured pre-chilling (22–25°C day/13–15°C night) and after 7 and 14 days of chilling (12–13°C day/7–9°C night). A different letter indicates significant difference ($p<0.05$). The data show the photosynthetic rate at a photosynthetic photon flux density of 1,000 μmol m^{-2} s^{-1} (A_{1000}).

Table 1. Recovery of the photosynthetic rate after chilling treatment

Clone	A_{1500} (μmol m^{-2} s^{-1})[1]		
	Pre-chilling[2]	Chilling 4 days[3]	Recovery 7 days[4]
JM14-09	28.8 b[5]	17.1 (59) ab	29.9 (104) a
JM14-72	33.2 a	14.8 (45) b	25.4 (77) b
JM14-88	23.4 c	13.2 (56) b	24.0 (103) b
KR05-619	28.3 b	9.3 (33) c	20.5 (72) c
KY06-139	29.3 b	9.5 (32) c	20.3 (69) c
Shiozuka	24.2 c	16.0 (66) b	24.9 (103) b
Miyakonojo	29.9 b	19.7 (66) a	28.9 (97) a

1) The photosynthetic rate at a photosynthetic photon flux density of 1,500 μmol m^{-2} s^{-1}. 2) Photosynthetic rates were measured five weeks after planting (26°C/18°C day/night). 3) Photosynthetic rates were measured after 4 days of chilling treatment (12°C day/7°C night). 4) Photosynthetic rates were measured after 7 days of recovery treatment (26°C day/18°C night). 5) A different letter indicates significant difference among the treatments ($p<0.05$). The values in parentheses in the table indicate the ratio to the photosynthetic rate of pre-chilling.

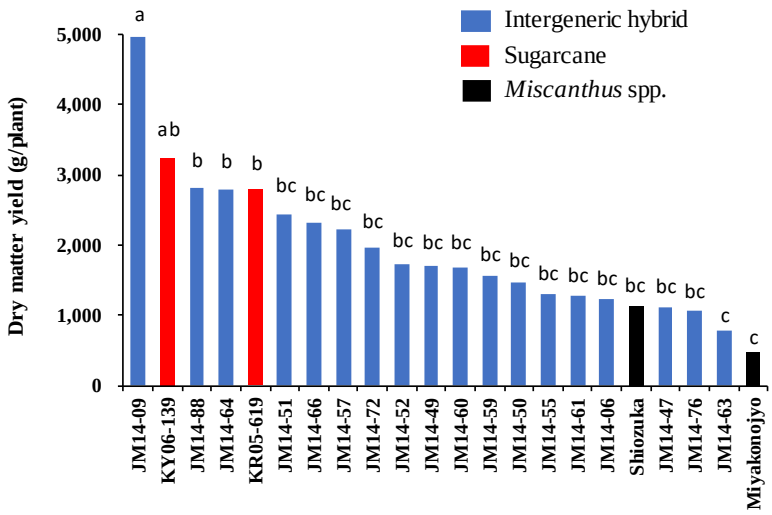

Fig. 2. Dry matter yield per year in the cold-climate region

The experiments were conducted for two years, in 2017 and 2018, at the fields in Hokkaido University (Sapporo, Japan: 43°07′N, 141°33′E). The experimental materials were planted in May and harvested in November, and the experimental plots were three replications with one plant per plot. The average temperature and precipitation in the experimental period were 17–18°C and 700–800mm, respectively. A different letter indicates significant difference ($p<0.05$).

Harunoogi, a high ratoon yield sugarcane cultivar developed by interspecific hybridization between sugarcane and *Saccharum spontanium*

Sugarcane (*Saccharum* spp. hybrid) is an essential crop for food and energy production, and improvement of its productivity will contribute toward promoting food sustainability and energy security around the world. Sugarcane can continue growing by low-cost cropping type ratooning, whereby the post-harvest stubbles in the fields are regrown. Improving ratoon productivity for high-latitude production areas, where low temperatures cause problems in ratooning, have been one of the most important breeding targets; however, the stagnation of genetic improvement arising from the narrow genetic diversity of cultivars and breeding materials in the world has become an issue in breeding, hence expanding genetic diversity using unused genetic resources is required. The wild sugarcane, *S. spontaneum*, is an important genetic resource for improving sugarcane ratoon yield due to its superior tillering and ratooning ability under various environments. The aim of this study therefore was to develop a sugarcane cultivar with good tillering ability and high ratoon yield for high-latitude sugarcane production areas by interspecific hybridization between sugarcane and *S. spontaneum*.

The new high ratoon yield cultivar Harunoogi was developed from a crossing between fodder sugarcane cultivar KRFo93-1 (which was developed by interspecific hybridization between sugarcane cultivar NCo310 and *S. spontaneum* Glagah Kloet and has excellent tillering ability with high ratoon yield at multiple ratooning) and the high-sugar-content sugarcane cultivar NiN24 (Fig. 1, Fig. 2). Harunoogi can produce an extraordinarily large number of stalks with sugar content comparable to that of NiF8, which is a major cultivar in high-latitude areas in Japan, even though its stalk diameter is smaller than NiF8 (Table 1). Its excellent ratooning ability enables the production of more stalks than NiF8 in ratoon crop, especially after machine harvesting (Fig. 3). As a result, cane yield and sugar yield in 1st and 2nd ratoon crops of Harunoogi are much higher than NiF8's (Table 1).

Harunoogi, which was jointly developed by the Japan International Research Center for Agricultural Sciences and the National Agriculture and Food Research Organization, is expected to contribute to sugarcane production in high-latitude areas in Japan. Interspecific hybridization with *S. spontaneum* will be an important strategy toward improving the tillering ability and productivity of ratoon crops in high-latitude areas where low temperature is a critical constraint in sugarcane production.

(Y. Terajima, A. Sugimoto, T. Hattori [NARO], M. Matsuoka [NARO], T. Terauchi [NARO], T. Sakaigaichi [NARO], S. Ishikawa [NARO], M. Tanaka [NARO], Y. Tarumoto [NARO], M. Hayano [NARO], K. Adachi [NARO], M. Umeda [NARO])

Japan International Research Center for Agricultural Sciences

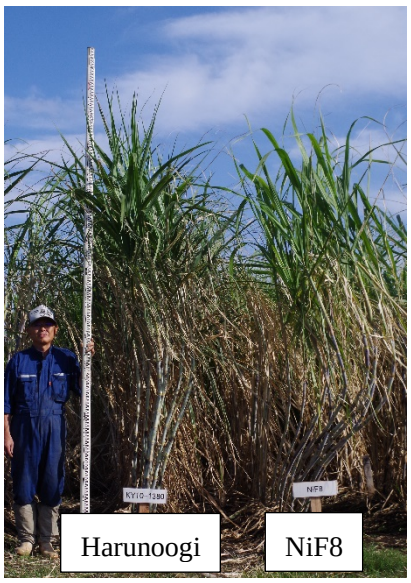

Fig. 1. Harunoogi and NiF8
Photos taken in November 2018
in Nishinoomote, Japan

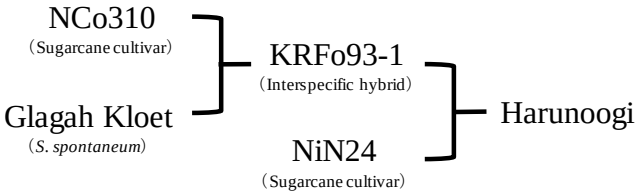

Fig. 2. The pedigree of Harunoogi

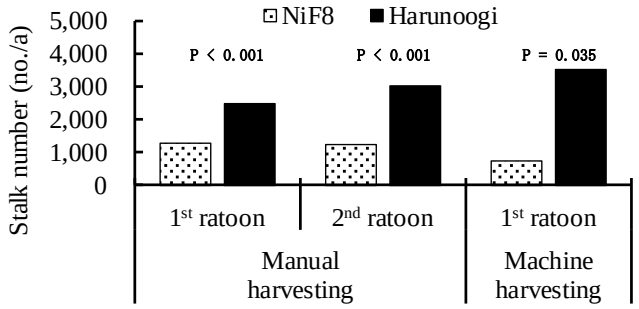

Fig. 3. Stalk number in early growth stage of the ratoon crop
The *p*-values were calculated by a generalized linear model with cultivar (fixed effect) and plot (random effect).

Table 1. The agronomic characteristics of Harunoogi

Cropping type	Cultivar	Stalk number (no./ha)	Stalk length (cm)	Stalk diameter (mm)	Single stalk weight (g)	Cane yield (t/ha)	Sugar content (%)	Sugar yield (t/ha)
New planting	Harunoogi	143,950	224	20.6	685	97.3	12.4	11.0
	NiF8	93,100	244	22.5	818	75.6	12.1	8.4
	p -value	<0.001	<0.001	<0.001	<0.001	<0.001	0.441	<0.001
1st ratoon	Harunoogi	188,667	244	19.4	619	117.2	11.8	12.7
	NiF8	110,633	238	20.5	649	71.9	12.4	8.2
	p -value	<0.001	0.272	0.016	0.337	<0.001	0.098	<0.001
2nd ratoon	Harunoogi	192,950	218	19.6	583	109.7	10.4	9.8
	NiF8	134,800	215	20.5	558	74.6	10.4	6.7
	p -value	0.003	0.733	0.116	0.492	<0.001	0.723	0.003

The experiments were conducted from 2015 to 2018 at Kyushu Okinawa Agricultural Research Center, Tanegashima Sugarcane Breeding Site, Nishinoomote, Japan. The results in the table show the means of 4 years (2015-2018) in new planting, three years (2016-2018) in 1st ratoon, and two years (2017-2018) in 2nd ratoon. The *p*-values were calculated by a generalized linear model with cultivar (fixed effect), year, and plot (random effect).

Current status of insecticide use by farmers for controlling rice planthoppers in the northern part of Vietnam

Insecticides are widely used in Asia to control insect pests on rice such as the rice planthoppers *Nilaparvata lugens* and *Sogatella furcifera*. It has been known that these species developed resistance against several insecticide ingredients, resulting in difficulty to control. They migrate from the central and northern parts of Vietnam to Southern China and Japan every year but are unable to overwinter in the immigrated areas. Hence, insecticide use in the source areas is a key factor when considering insecticide resistance management. Here we investigated the situation of insecticide use by local rice farmers and the effect of insecticide application to the density of planthoppers in the northern part of Vietnam.

Interviews with rice farmers revealed the active ingredients used in the paddy fields. Ten groups consisting of 21 ingredients were confirmed in two villages in Nam Dinh and Vinh Phuc Provinces, with the differences noted among locations and crop seasons (Table 1). Generalized linear model analysis was performed, with locations, crop seasons, the applied number of insecticide ingredients, and the number of spiders and mirid bugs (the natural enemies of planthopppers) as explanatory variables, and the planthopper density at booting stage as response variable. The results indicated that the applied number of ingredients has a weak effect in reducing the density of planthoppers (Table 2). Pesticide application using knapsack sprayers was evaluated using water-sensitive papers (WSPs). Droplet depositions on WSPs were high at the top part of the rice plant (height above the water surface ≈ 60 cm), moderate at the middle part (40 cm) where *S. furcifera* lives, and low at the bottom part (15 cm) where *N. lugens* lives (Fig. 1). The mortality of adult female *N. lugens* was high when the droplet deposition rank was high (Fig. 2), implying that one of the factors for the weak effect of insecticide application by farmers was that insecticide droplets did not reach the targets' habitats.

The results indicated that improving the method of pesticide application, i.e., enabling the droplets to reach the planthoppers' habitat, will efficiently control rice planthopper because, in general, systemic insecticides are rarely transferred from the top to the bottom of the plant. Insecticide resistance development is probably another reason for the lower efficiency in pest control. Vietnamese planthopper population needs to be monitored for insecticide resistance.

(M. Matsukawa, Y. Kobori, C. H. Nguyen [Plant Protection Research Institute])

Table 1. Insecticide ingredients used by farmers in two villages in Northern Vietnam

Group	Active ingredients	Nam Dinh		Vinh Phuc	
		Winter (38)	Summer (38)	Winter (37)	Summer (26)
Average frequency of spraying the active ingredients/field		4.48	8.83	0.29	1.88
Carbamates	BPMC	-	-	-	○
Organophosphates	Chlorpyrifos	○	-	-	○
	Chlorpyrifos-ethyl	○	○	-	○
	Quinalphos	○	○	-	-
Phenylpyrazoles	Fipronil	○	○	○	○
Pyrethroids	Cypermethrin	○	○	-	○
	Permethrin	-	○	-	○
	lambda-Cyhalothrin	○	-	-	-
	alpha-Cypermethrin	○	○	-	-
Neonicotinoids	Imidacloprid	○	○	-	-
	Nitenpyram	○	-	-	-
	Acetamiprid	-	○	-	-
	Dinotefuran	-	○	-	-
	Thiamethoxam	-	-	○	○
Avermectins	Abamectin	○	○	-	○
	Emamectin benzoate	○	○	-	○
Pyridine azomethine derivatives	Pymetrozine	○	○	○	-
Nereistoxin analogues	Thiosultap-sodium	-	○	-	-
Buprofezin	Buprofezin	○	○	-	-
Oxadiazines	Indoxacarb	○	○	-	-
Diamides	Chlorantraniliprole	-	○	○	○

Active ingredients were classified by the Insecticide Resistance Action Committee. The number in the parenthesis is the number of farmers interviewed.

Table 2. Results of generalized linear model analysis on variables affecting the density of rice planthoppers

Explanatory variables	d.f.	Estimated value	χ2	p value
Location	1	0.63	4296.03	<0.001
Crop season	1	-0.31	662.63	<0.001
Applied number of ingredients	1	0.02	22.47	<0.001
Number of spiders	1	0.02	4534.75	<0.001
Number of mirid bugs	1	0.06	6285.56	<0.001

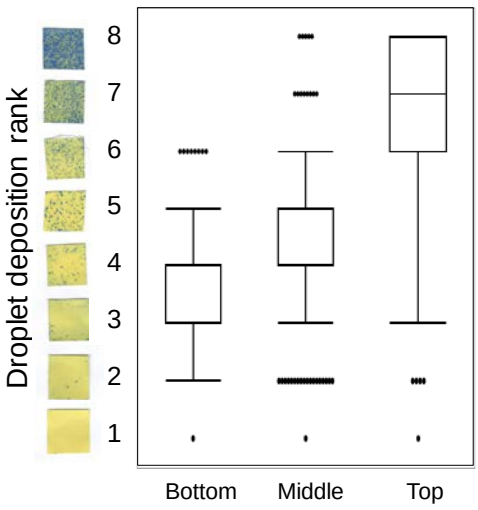

Fig. 1. Droplet deposition ranks at different heights of the rice plant

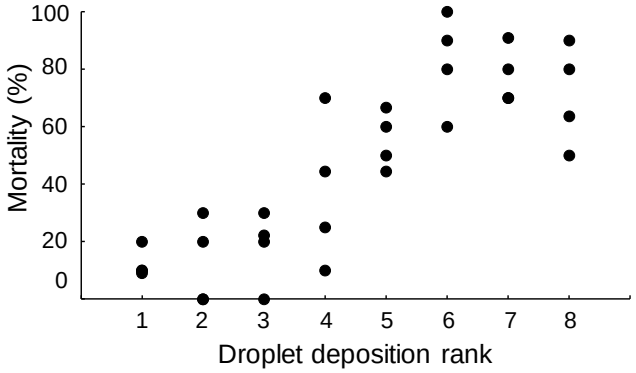

Fig. 2. Relationship between the droplet deposition rank and mortality of *N.lugens*

Dots show the mortality for each replicate. Insecticide contains 45% nitenpyram, 25% pymetrozine, and 5% imidacloprid (w/w).

Liquefaction of Thai fermented rice noodles can be prevented by maintaining the product in acidic condition of pH around 4

Fermented rice noodles, traditionally known as *khanom jeen* in Thailand, are produced and consumed countrywide. Similar types of products are common in Laos, Vietnam, Cambodia, Myanmar, and China. *Khanom jeen* is made from fermented rice flour containing lactate. In the noodle factories, the fermented rice flour is heated to achieve partial starch gelatinization and kneaded with water. The dough is then extruded into noodles in boiling water for about one minute, washed with water, drained using a sieve container, and sold. The fermented rice noodles have a unique and preferable flavor and texture achieved through the rice fermentation process. Normally, the products retain quality without rotting for a few days at ambient temperature. Refrigeration is not applicable to the noodles because starch retrogradation at cold temperatures ruins the unique texture. However, it occasionally suffers from severe liquefaction (Fig. 1) before the products are sold in the market. Although the direct cause has yet to be clarified, an urgent solution to the liquefaction problem is needed to reduce economic and food losses.

Liquefaction is thought to result from water release associated with digestion of the starch maintaining the noodle structure by amylolytic enzymes with pH preferences for activity. The fermented rice noodles containing 0.03% lactate is acidic with a pH of 3.7. The pH changes to 4.0, 6.0, or 7.7 after soaking in McIlvaine buffers at pH 4.0, 6.0, or 8.0 for 10 min, respectively. Moisture transudation and partial liquefaction are observed in noodles treated with buffers at pH 6.0 or 8.0 after 3 to 5 days of incubation at 37°C (Fig. 2). In contrast, such phenomena are not observed in noodles treated with buffer at pH 4.0 (Fig. 2) or in those treated with buffer containing 200 μg/mL chloramphenicol (data not shown), indicating that liquefaction of fermented rice noodles is induced, accompanied by bacterial growth in products in which the pH is heightened to 6.0 or higher. α-amylase activity is detected in noodles treated with buffers at pH 6.0 or 8.0 after 2 days or 1 day of incubation, respectively (Fig. 3A). An increase in reducing sugar is observed in accordance with α-amylase production under liquefaction-inducing conditions (Fig. 3B). It is presumably derived from oligosaccharides by starch digestion in noodles. Taken together, it is important for the producers to maintain fermented rice noodles as well as fermented rice flour in acidic condition of pH around 4 to prevent liquefaction of the products.

The producers can monitor the pH of their products by using a food-grade pH meter or with the simplified method using pH-test papers. It is also recommended that the producers check the pH of the water for washing the fermented rice noodles at the end of production. Underground water, which is generally used for the washing stage, might be alkalized due to soluble minerals. Edible organic acids such as acetate can be used to adjust the pH of the washing water, although the usage needs to be carefully optimized in consideration of the flavor of the product. Information regarding liquefaction prevention and the manufacturing process, as well as serving ideas for fermented rice noodles, are simply summarized in a booklet in Thai (Fig. 4). It would be useful not only to the producers but also the general public, and it is expected to increase productivity, improve the food value chain, and raise awareness on this great local food tradition.

(J. Marui, T. Yoshihashi, S. Shompoosang [IFRPD, Kasetsart University],
V. Surojanametakul [IFRPD, Kasetsart University])

Fig. 1. Liquefaction of fermented rice noodles

Fig. 2. Appearance of fermented rice noodles after 3 and 5 days of incubation at 37°C after soaking treatment with McIlvaine buffers at pH 4.0, 6.0, and 8.0

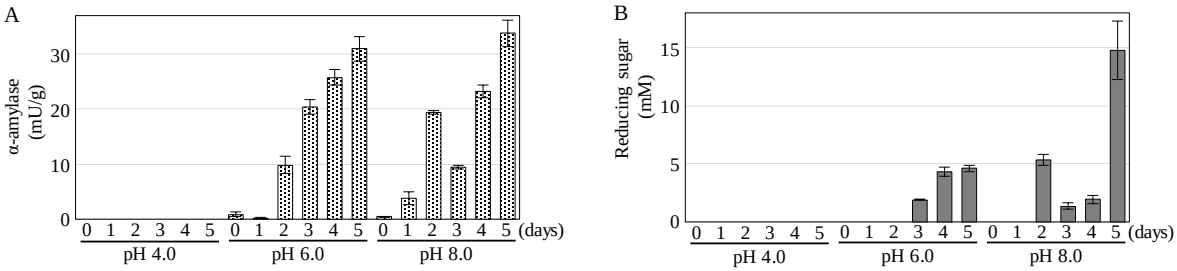

Fig. 3. Time-dependent change in α-amylase activity (A) and reducing sugar content (B) in fermented rice noodles treated with McIlvaine buffers at pH 4.0, 6.0, and 8.0

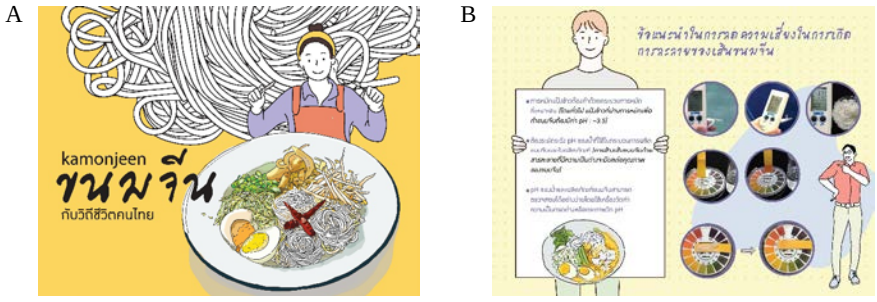

Fig. 4. Cover illustration (A) and introduction of pH monitoring methods (B) in a booklet on fermented rice noodles, written in Thai

New approach for Tartary buckwheat utilization by rapid heating treatment

Tartary buckwheat (*Fagopyrum tataricum* Gaertn.) is widely known as a functional food/medicinal source throughout the world. A relatively low-demanding crop, Tartary buckwheat can tolerate environmental stresses such as water deficiency, diseases, insects, and ultraviolet radiation, thus it is often used in organic farming systems and as an emergency crop around the world. Tartary buckwheat is anticipated to be utilized for various food products due to its high rutin content, indicating high potential in terms of functional benefits. However, its utilization is limited owing to the difficulty in dehulling its hard pericarp and the strong bitterness of its products, which in turn are attributed to quercetin formation by rutinosidase-induced rutin hydrolysis in buckwheat seed. In addition, enzyme activity in Tartary buckwheat is strong enough to hydrolyze rutin to quercetin in a very short time, comparable with that of common buckwheat. Thus, products using Tartary buckwheat as an ingredient are strongly bitter in taste even if mixed with common buckwheat, which is otherwise not bitter.

This study therefore aimed to develop an effective treatment to overcome both the limitations of dehulling and rutinosidase activity in Tartary buckwheat utilization by circulated fluidized-bed heating. Using a circulated fluidized-bed at high temperatures, the treatment enabled buckwheat to produce a popcorn-like gelatinized product (Fig. 1). Also, although rutin was mostly retained in the samples, the products did not exhibit bitterness and their functionality was conserved (Table 1). Owing to the denaturation of rutinosidase in the heat-treated products, rutin content in the model system (i.e., Tartary buckwheat mixed with common buckwheat) was retained without the formation of the bitter digested product, quercetin (Fig. 2). Nutritional analysis of pre- and post-treated products showed retention of the macronutrients even after heat treatment. The popped Tartary buckwheat could, therefore, be obtained by simple treatment, and might reveal new opportunities to utilize pre-gelatinized and rutin-rich properties by rutinosidase denaturation (Table 2).

Regarding this treatment’s utilization and future prospects, its biggest advantage is that it broadens the utilization of Tartary buckwheat as a simple and low-cost functional food source. The final edible product contains high rutin without bitterness and rutinosidase activity. Furthermore, the model study showed the possibility of using the popped Tartary buckwheat as an intermediate product, providing high amounts of rutin to various foods, such as bread, steamed bun, and buckwheat noodle, as a mixture ingredient. The treatment curtails production cost by rapid heating in a circulated fluidized-bed, and it does not require high-pressure processing.

(K. Fujita, T. Yoshihashi)

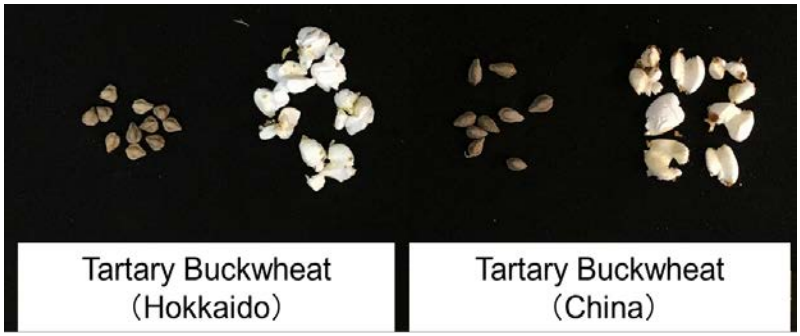

Fig. 1. Popped Tartary buckwheat using circulated fluidized-bed heating treatment
The treatment provides edible popped Tartary buckwheat in a short time.

Table 1. Rutin content of samples with/without the treatment (dry matter basis)

Sample name	Treatment	Rutin (mg/100g)
Tartary buckwheat (Hokkaido)	Unpopped	1,637±118.2
	Popped	1,469±49.5
Tartary buckwheat (China)	Unpopped	1,548±77.8
	Popped	1,202±72.2

Rutin was slightly decreased; however, the product did not show bitterness from the rutin-degraded product, quercetin.

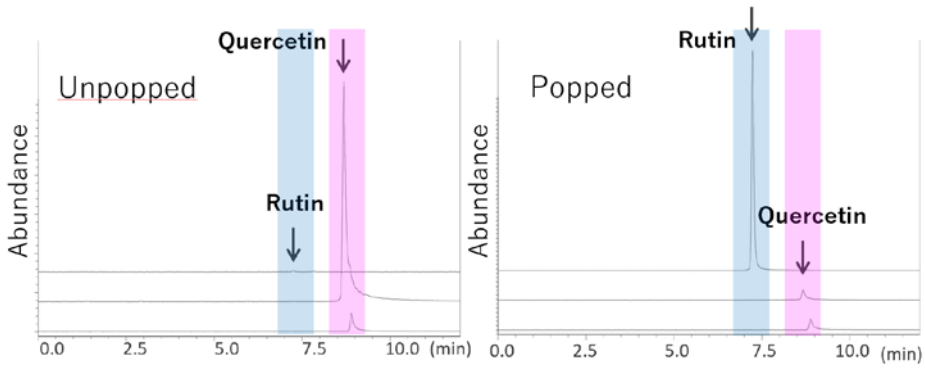

Fig. 2. Chromatograms of rutinosidase assay mixtures using crude enzymes
The assays were performed with crude enzyme from Tartary buckwheat samples with rutin, then the substrate (rutin) and product (quercetin) were quantified.

Table 2. Macronutrients in Tartary buckwheat samples (Hokkaido)

Sample name	Treatment	Protein (g/ 100g)	Fat (g/ 100g)	Ash (g/ 100g)	Carbohydrate (g/ 100g)	Fiber (g/ 100g)	Energy (kcal/ 100g)
Tartary buckwheat (Hokkaido)	Unpopped	13.7	4.1	2.3	79.9	5.7	411
	Popped	12.5	4.0	2.2	81.3	4.5	411

Main factors that determine the amounts of soluble sugar and starch in old oil palm trunk

Palm oil occupies 40% of global vegetable oil production, with 85% of all palm oil production confined to a restricted area that is primarily within Indonesia and Malaysia. Oil palm stem contributes a large proportion of the waste, but its sap contains approximately 11% soluble sugar. Non-structural carbohydrates (NSC), including soluble sugars and starch in the stem, can be used as a substrate in bioreactors and so on. Although soluble sugar content in the sap of felled trunk was identified to be dependent on the amount of starch (JIRCAS Research Highlights 2017, C07), the mechanisms through which NSC accumulate in the stem have not yet been well documented. Oil palm cultivation is limited in the surrounding area of the equator, hence it has been considered that water stress due to high temperature and drought affects productivity of fruit bunches, which leads to the seasonality of production. Here, we investigated how environmental conditions influence NSC in stem and fruits as intermediate and final storages. These findings should contribute to the stable production of palm oil as well as the utilization of NSC from the stem in downstream applications.

The volume of fruit bunch increased from around October, reaching maximum around May the following year, then matured fruit bunches dropped. Increments in soluble sugar levels were observed but increments in starch levels were not obvious during periods when there were less fruit bunches (Fig. 1). Convergent cross mapping (CCM), an analytical method in empirical dynamic modeling to identify causal relationship between time-series showing non-linear dynamic, showed a causal relationship between soluble sugar in stem and volume of fruit bunch. Furthermore, CCM showed that the 60-day cumulative temperature taken backward from the observation dates (CT) was causally and strongly related to soluble sugar and starch in stem with about a half-year time lag, but not to volume of fruit bunch. Similarly, 60-day cumulative rainfall taken backward from the observation dates (CR) was causally related to soluble sugar and starch in stem with no time lag (Fig. 2).

The above results suggest that the main factors that determine soluble sugar and starch in the stem are temperature and subsequently rainfall fluctuations. The period from October to December, when lower temperatures and higher cumulative rainfall are observed in the northern part of Malay peninsula where the study was conducted, was identified as the period with maximum stem NSC stocks. This finding can contribute to planning the timing of tree felling operations to maximize soluble sugar and starch in old oil palm stem for downstream usage in biorefineries. When the finding is applied to other regions, it is necessary to identify environmental factors indicating strong causality and its time lags.

(N. Tani, A. Kosugi, T. Arai, T. Kondo, Z. A. Abdul Hamid [Universiti Sains Malaysia (USM)], N. Joseph [USM], O. Sulaiman [USM], R. Hashim [USM], A. Satake [Kyushu University])

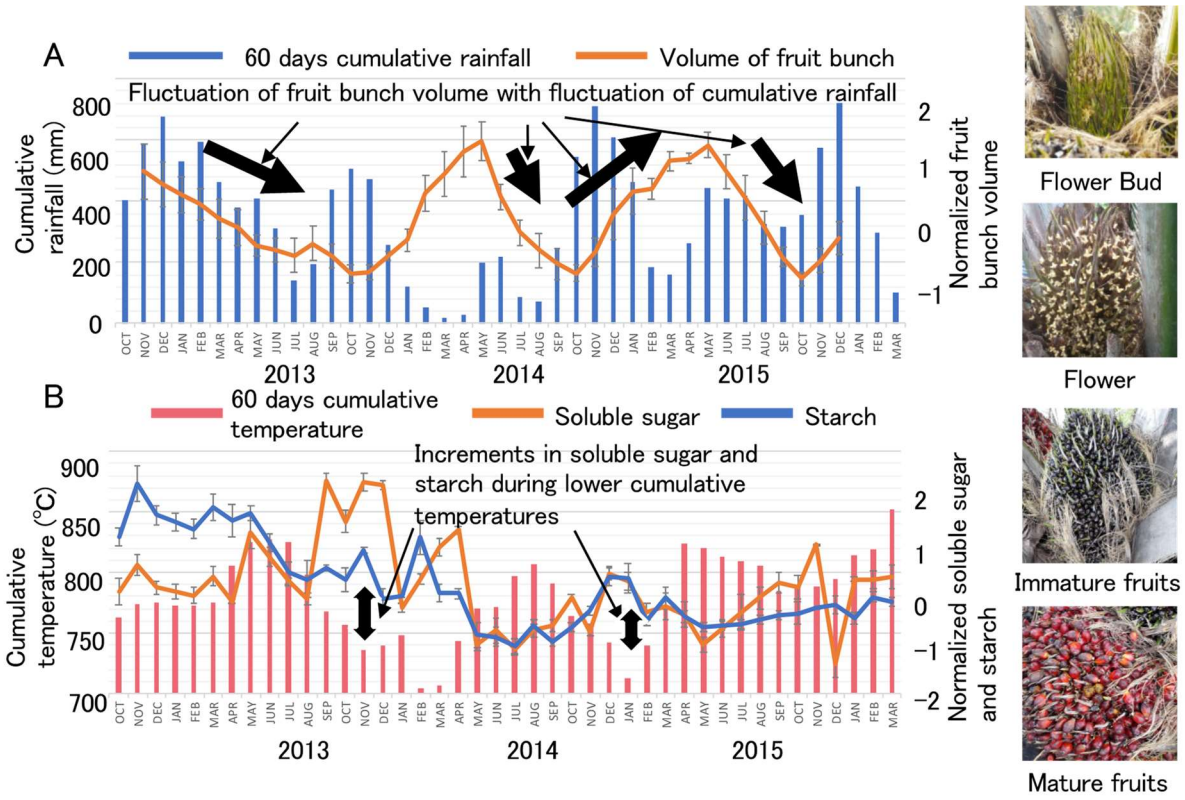

Fig 1. The volume of fruit bunch summed from all development stages, shown by photos on the right side, and 60 days cumulative rainfall (A), the amounts of soluble sugar and starch in oil palm stem and 60 days cumulative temperature during the observation period (B)

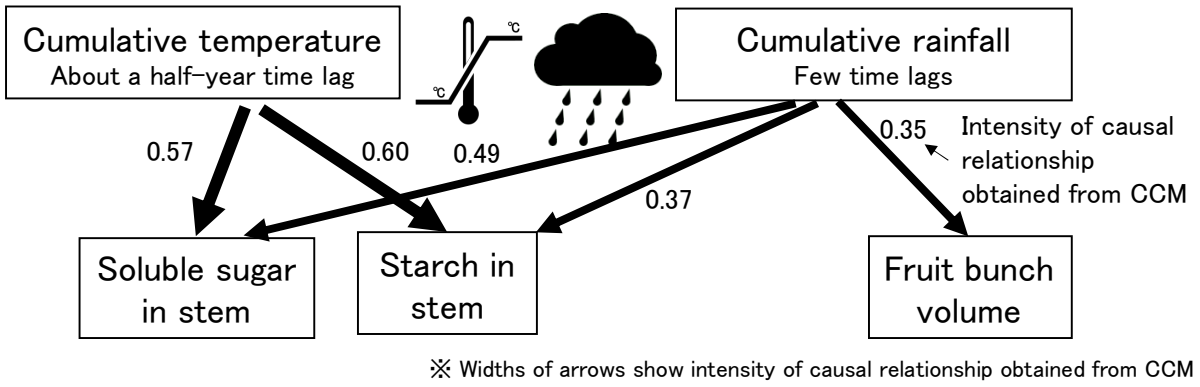

Fig. 2. Significant causal relationship from cumulative temperature and rainfall to soluble sugar, starch in oil palm stem, and volume of fruit bunch evaluated by empirical dynamic modelling

Bacillus aryabhattai produces bioplastics from starch in agricultural residues

In Southeast Asia, large amounts of agricultural residues such as cassava pulp and oil palm trunk are generated, causing various environmental problems. On the other hand, starch that remained in crop residues is considered as a useful biomass resource. In recent years, the harmful effect of petroleum-based plastics on the environment has been raised in global discussions. Polyhydroxybutyric acid (PHB), a bioplastic material, is expected to become a substitute for petroleum plastics. However, there are some challenges that prevent its widespread use. One big problem is its high production cost, half of which is due to the price of the substrate. The aim of this study, therefore, was to screen for bacteria that can produce PHB, using starch from agricultural waste, in a single step.

Eighty-four (84) strains of PHB-producing bacteria were isolated from Japanese soil, and *Bacillus aryabhattai*, the bacterium that produced the largest amount of PHB, was isolated from the screening medium. Because *B. aryabhattai* retains an amylase gene (*amyA*), starch can be degraded into glucose by the amylase secreted outside the cells, and the glucose is used as a feed resource to produce PHB and accumulate PHB granules in the cells. When the bacteria were cultured using soluble starch as a carbon source (under optimum conditions considering temperature, pH, starch concentration, etc.), the cell weight was 4.4 g/L, PHB content in cells was 46%, and PHB production was 1.9 g/L.

The above data show that the bacteria exhibit high efficiency in producing PHB from soluble starch (Fig. 1). On the other hand, *Cupriavidus necator*, which has been used industrially as a PHB-producing bacterium, cannot use starch because it has no amylase gene and cannot produce PHB even when cultured under the same conditions (Fig. 1). When *B. aryabhattai* was cultured using cassava pulp or starch from oil palm trunk as a carbon source, the cassava pulp starch was degraded by 96% and the oil palm trunk starch by 99%. PHB production was 0.12 g/L and 0.33 g/L, respectively (Fig. 2, Table 1). The weight-average molecular weight, which indicates the physical properties of PHB, was the same as PHB produced using commercially available glucose as a carbon source (Table 2). The melting point, an indicator of heat resistance, was higher than that of PHB produced using commercially available glucose as a carbon source. From these results, the *B. aryabhattai* PHB is expected to be suitable for heat processing at high temperatures and for increasing the heat resistance of the product.

By using *B. aryabhattai*, PHB can be produced directly from starch in agricultural residues of cassava pulp and oil palm trunk without using starch-degrading enzymes, thereby reducing the cost of bioplastic production. A reduction in environmental load can be also expected.

(*T. Arai, A. Kosugi, S. Sudesh [Universiti Sains Malaysia]*)

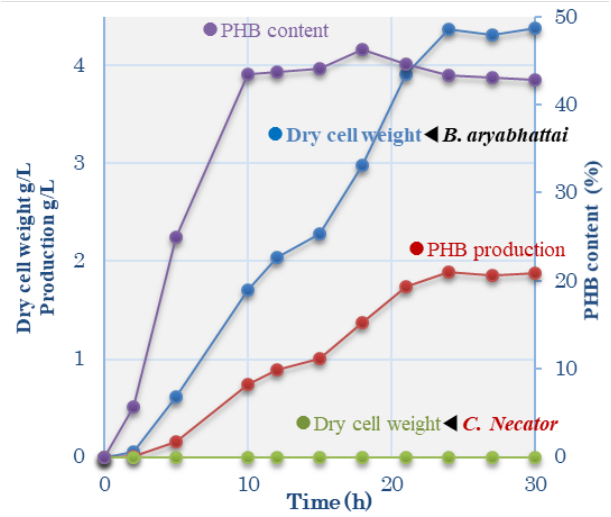

Fig. 1. PHB production from soluble starch by *B. aryabhattai*

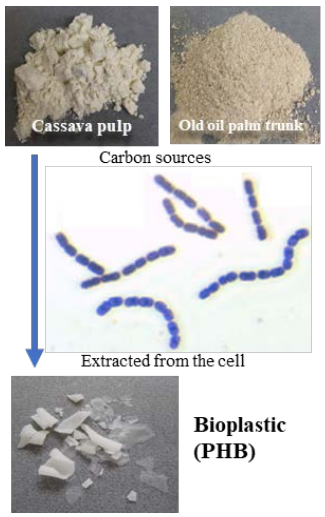

Fig. 2. PHB production from starch in agricultural waste and residues

Table 1. PHB production from unused starch in crop residues by *B. aryabhattai*

Source of starch	Starch degradation (%)	Dry cell weight (g/L)	PHB production (g/L)	PHB content (%)
Cassava pulp	96±3	1.42±0.08	0.12±0.03	8.68±1.44
Old oil palm trunk	99±1	1.95±0.05	0.33±0.06	17.07±2.83

Table 2. Physical property ratio of PHB produced from glucose and cassava pulp by *B. aryabhattai* and other bacteria

Strain	Carbon source	Physical properties of PHB		
		Weight - average molecular weight	Number average molecular weight	Melting point (℃)
B. aryabhattai	Glucose	2.19×10^5	4.43×10^4	165
	Cassava pulp	1.61×10^5	4.28×10^4	170
Bacillus spp. 871	Glucose	5.13×10^5	Unmeasured	153
Bacillus spp. 112A	Glucose	5.21×10^5	Unmeasured	148
Saccharophagus degradans	Glucose	5.42×10^4	Unmeasured	166

Efficacy of black soldier fly larvae as a protein source in aquaculture feed for the climbing perch

In Laos, demand for food fish has been increasing in recent decades, with the promotion of aquaculture playing a key role in the government's national population development strategy. However, aquaculture feed procurements have been entirely dependent on imports from neighboring countries, resulting in high costs causing limitation of broad extension of aquaculture in the country. In addition, protein content in aquaculture feeds is highly dependent on fishmeal (FM), and price fluctuations in FM largely affect the current/future price of feeds. With this background, the identification of substitutional protein sources becomes important in reducing feed costs and dependence on FM. Here, we evaluated the efficacy of black soldier fly (*Hermetia illucens*, referred to as BSF) larvae (Fig. 1a) as a protein source in aquaculture feed for the climbing perch (*Anabas testudineus*) (Fig. 1b).

The BSF larvae were cultured beforehand with feeding on fruit residues and beer draff. Three different feeds (with/without BSF larvae) were prepared as follows: feed T1 (the control feed) with the highest crude protein (CP 32.5%) using only FM as animal protein source; T2 as the lower protein feed (CP 30.0%) using FM/BSF mixed meals; and T3 as the lowest protein feed using only BSF (CP 25.0%) (Table 1).

After 123 days of culture trials using the above feeds, major growth indices (total length, body weight, survival rate, and feed conversion ratio) in fish given the feeds T2/T3 were not significantly different from those of fish given the T1, although the CP levels in the T2/T3 were lower than that in the T1 (Table 2). In addition, the protein efficiency ratio (PER) was significantly higher in fish given the feed T3 than that of fish given the T1/T2, and the protein retention (PR) was higher in fish given the T3 than that of fish given the T1 (Table 3). These results strongly indicate that the protein in BSF larvae is more assimilative for the climbing perch than that in FM.

The above results show that BSF larvae are a promising feed protein source for climbing perch aquaculture and have the potential to reduce dependency on FM, leading to feed cost reduction. Better protein assimilation of BSF larvae by the climbing perch is probably attributable to the feeding habit of the climbing perch, which is an insectivore. Therefore, the efficacy of BSF larvae on other fishes with different feeding habits should be validated separately.

(S. Morioka, B. Vongvichith [Living Aquatic Resources Research Center])

Fig. 1. Black soldier fly larvae (a) and the climbing perch (b)

Table 1. Proximate contents of the experimental feeds T1-T3 (% dry matter)

Feed	T1	T2	T3
Crude protein	32.5	30.0	25.0
Crude fat	6.7	7.6	8.9
Crude ash	11.1	9.5	7.3
Crude starch	22.8	28.0	27.7

Table 2. Growth performance of the climbing perch given the experimental feeds T1, T2 and T3

Growth index	T1	T2	T3
Total length at stocking (mm)*	46.3 ± 7.4	46.3 ± 7.4	46.3 ± 7.4
Total length at harvest (mm)**	159.9 ± 13.6	164.1 ± 11.7	160.9 ± 12.8
Body weight at stocking (g)*	2.2 ± 1.2	2.2 ± 1.2	2.2 ± 1.2
Body weight at harvest (g) **	85.1 ± 25.5	92.0 ± 22.3	83.5 ± 22.2
Survival rate (%)***	82.2 ± 2.0	81.7 ± 9.1	81.7 ± 2.9
Feed Conversion Ratio***	3.4 ± 0.2	3.2 ± 0.4	3.2 ± 0.1

Values are the mean ± standard deviation, *n = 180, **n = 60, ***n = 3

Table 3. Proximate contents of fish body reared by the feeds T1, T2 and T3 (moisture, crude protein, crude ash), and indices of protein assimilation (protein efficiency ratio, protein retention)

Contents	At stocking	At harvest		
		T1	T2	T3
Moisture	77.6 ± 0.2 (6)	63.4 ± 1.5 (18)	62.8 ± 1.0 (18)	63.1 ± 0.8 (18)
Crude protein	14.9 ± 0.3 (6)	18.1 ± 0.3 (6)	17.8 ± 0.8 (6)	17.2 ± 0.6 (6)
Crude fat	2.8 ± 0.1 (6)	12.0 ± 0.9 ^{a} (12)	12.3 ± 1.7 ^{a} (12)	14.4 ± 2.2 ^{b} (12)
Crude ash	3.8 ± 0.6 (6)	5.4 ± 1.0 ^{a} (18)	5.7 ± 0.7 ^{a} (18)	4.1 ± 0.8 ^{b} (18)
Protein assimilation indices		T1	T2	T3
Protein efficiency ratio		**0.9 ± 0.1 ^{a} (3)**	**1.1 ± 0.1 ^{a} (3)**	**1.3 ± 0.1 ^{b} (3)**
Protein retention		**16.4 ± 0.7 ^{a} (3)**	**18.8 ± 2.3 ^{a,b} (3)**	**21.9 ± 0.8 ^{b} (3)**

*Values are the mean ± standard deviation, *numbers in parentheses are the number of samples.
** Different capital letters indicate significant difference (Tukey's HSD test, $p < 0.05$).

Biological information contributing to resource conservation of the important Laotian food fish *Pa keo*

Pa keo (*Clupeichthys aesarnensis*), a small-sized clupeid fish (Fig. 1) that is widely distributed in the Indochinese Peninsula, is an important food fish over the area, including Laos. It is captured in great quantities mainly from large-scale man-made reservoirs such as the Nam Ngum Reservoir in Laos, and consumed as dried/fermented fish. In the recent decade, overexploitation/stock decline of this species as a food resource has become a matter of great concern, hence resource management is required.

Based on the above background, we attempted to investigate the population dynamics of *Pa keo* in Nam Ngum Reservoir by clarifying several biological features (e.g., the age in days and reproduction) in order to propose applicable resource management approaches for the species.

To determine the age in days by individual specimen, we analyzed the daily increments in the otolith (sagitta) (Fig. 1). On the basis of age information by individual specimen, we estimated the hatch month of each specimen and confirmed the year-round breeding of the species in the reservoir (Fig. 2). The relationship between gonadosomatic index [GSI = (weight of ovary/testis) / body weight × 100] and standard length (SL) indicated that the minimum maturation size was 28-30 mm SL for both females and males (Fig. 3), and the growth pattern was regressed by the von Bertalanffy growth curve [$Lt = 44.76 \cdot (1-\exp(-0.01 \cdot t))$, $R^2 = 0.89$, n = 486] (Fig. 4a). Based on this growth model, the theoretical maximum size of *Pa keo* population in the reservoir was estimated to be ca. 45 mm SL, and ages reaching first maturation (28-30 mm SL, Fig. 3) were estimated to be over 100 days old (Fig. 4a). In the analyzed specimens (n = 486), the specimens of 30-40 mm SL were the greatest in number followed by the ones of 20-30 mm SL (Fig. 4b). Although the maximum size of the species was reportedly over 70 mm SL, a limited number of specimens were over 50 mm SL in this study (0.4% of analyzed specimens). Considering this size distribution and the theoretical maximum size observed in this study (Fig. 4), the individual maximum size in this population was considered to become smaller over time. This down-sizing is considered the “evolutionary down-sizing” caused by consecutive catches of larger specimens and/or over-exploitation in the population, suggesting the necessity of *Pa keo* resource management in Nam Ngum Reservoir.

Since *Pa keo* breeds year-round (Fig. 2), setting up a “non-fishing area” is considered a more efficient manner of resource conservation than setting up a “non-fishing period” from the aspect of conserving the breeding population. In addition, in order to control the increasing fishing effort (i.e., number of fishermen and fishing gears), implementation of a fishing license system and/or a fishing restriction/gear control system should be considered.

(S. Morioka, J. Marui)

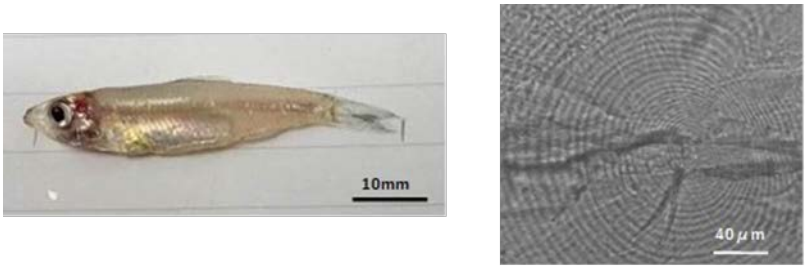

Fig. 1. Adult *Pa keo* (40 mm SL) (left) and daily increments in otolith (right)

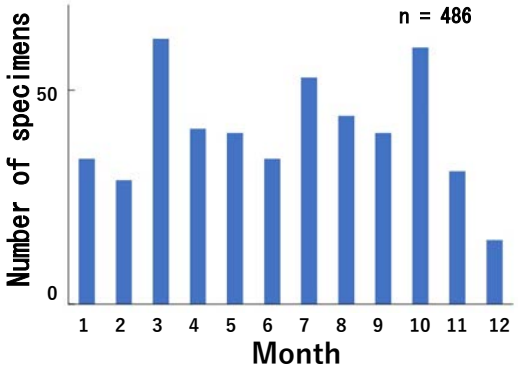

Fig. 2. Hatch month distribution

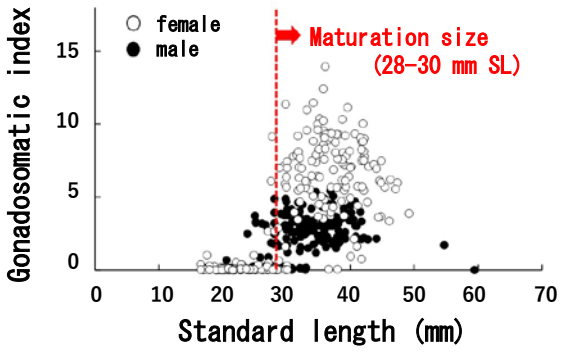

Fig. 3. Relationship between SL and GSI

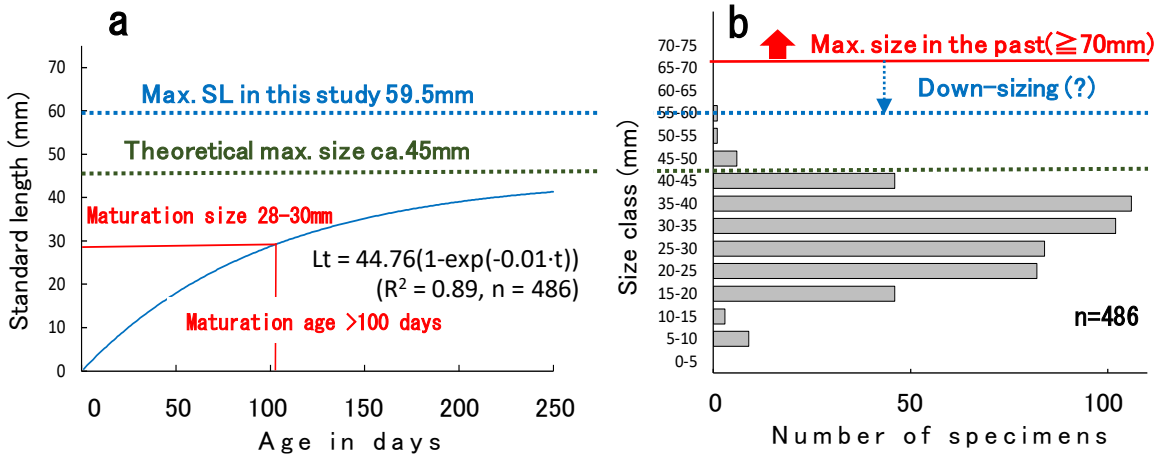

Fig. 4. Growth model of *Pa keo* population (a) and size frequency distribution (b)

Utilization of poultry by-product meal as an effective alternative to fish meal in aquaculture feed for milkfish *Chanos chanos*

In many cases, aquaculture feeds depend on fish-meal and fish-oil as their protein and fat sources, respectively. They are products of capture fisheries. The recent stagnation in capture fisheries production due to limitations on fisheries resources, has caused a steep rise in the price of fish-meal/fish-oil, and eventually aquaculture feeds, to fulfill increasing demands for aquaculture products. In the case of Philippine milkfish cage culture, feed cost covers three quarters of the total expenses. Thus, reducing feed costs is essential to improve profitability of aquaculture management. We explored possible alternative protein sources that are cheap, effective, and available on site to reduce dependency on fish-meal/fish-oil in producing fish feeds. In the Philippines, we developed low fish-meal feeds for milkfish by utilizing poultry by-products (PBP), which are wastes that are collected after removing the edible parts from poultry.

Replacing the fish-meal with PBP, the experimental feeds were formulated to contain 27% crude protein, 10% crude fat, and 31% crude starch (Table 1). Milkfish juveniles (≈50g) were fed with experimental feeds and grown to market size (≈300g). Among experimental feeds, there were no significant differences in the growth parameters such as weight gain, specific growth rate, feed conversion ratio, and survival rate of the milkfish (one-way ANOVA and Fisher's PLSD) (Fig. 2A). The plasma components (phospholipids, triacylglycerol, and total cholesterol) of the harvested fish were not significantly affected by the experimental feeds (Fig. 2B). The proximate compositions of dorsal muscle from harvested fish, such as crude protein, crude fat, ash, and moisture, were not significantly different from each other's (Fig. 2C), and so were those of the whole body and the liver. Regarding the taste of the harvested fish, 48 participants (common people and researchers) did not recognize the differences in terms of smell, taste, and textures of the fish, and whether which of the experimental feeds were fed. These results indicate that the low fish-meal/fish-oil feeds developed using PBP have equivalent effect as commercial feeds on the growth of the juvenile milkfish and the quality of the harvested fish. As a result, we can reduce fish-meal by 75% and fish-oil by 15% if we mix 12% PBP as feed raw material for milkfish aquaculture.

We have also evaluated the versatility of the developed PBP feeds, and noted that it could be utilized effectively not only to milkfish but also to other aquaculture fishes. However, as the proximate compositions of PBP differ a lot, the compound ratio of PBP for the feeds should be adjusted accordingly.

(T. Sugita [National Research Institute of Fisheries and Environment of Inland Sea, A. B. Gavile [Aquaculture Department, Southeast Asian Fisheries Development Center (SEAFDEC/AQD), Philippines], J. G. Sumbing [SEAFDEC/AQD])

Fig. 1. Harvested milkfish (*Chanos chanos*) 29.8 cm fork length

Table 1. Composition of the experimental feeds

	CTF	LPF	HPF
Poultry by product	0%	8%	12%
Fish meal	20%	10% (-50%)	5% (-75%)
Fish oil	4.45%	4.00% (-10%)	3.78% (-15%)

The parenthesis indicates reduction rate of fish meal and fish oil.

CTF: Control feed, LPF: Low poultry by-product feed, HPF: High poultry by-product feed

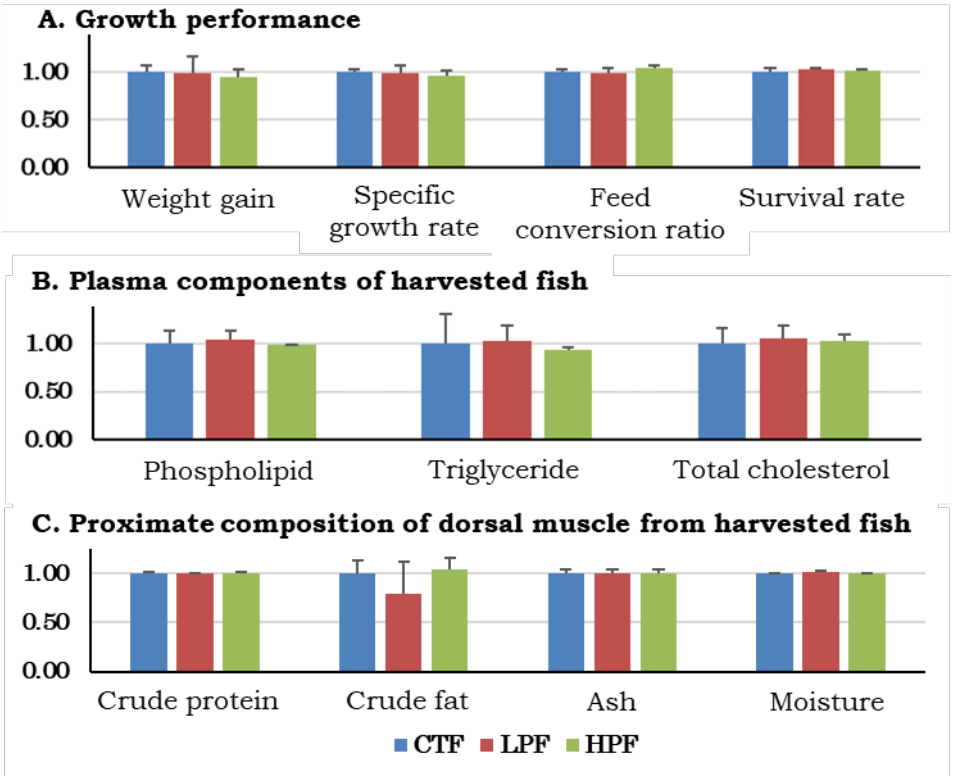

Fig. 2. Growth performance and quality of harvested milkfish fed with experimental feeds. Relative values when each value at CTF = 1.00. Initial number of experimental fish: 1483±1, Culture period: 84 days, Average water temperature: 28.3±1.2℃

A. Growth performance, B. Plasma components of harvested fish (N=10x2 replicates), C. Proximate composition of dorsal muscle from harvested fish (N=15x2 replicates)

Use of RNA interference to suppress gene expression of vitellogenesis-inhibiting hormone in the whiteleg shrimp, *Litopenaeus vannamei*

The shrimp culture industry continues to expand worldwide, and now boasts a production scale of over 5 million tons per year and market volume of nearly 30 billion U.S. dollars (FAO, 2019). In commercial shrimp hatcheries, eyestalk ablation is routinely performed because this procedure removes the source of vitellogenesis-inhibiting hormone (VIH) and allows ovarian maturation to proceed. However, it is currently viewed in the aquaculture industry that it is essential to develop a technology that could replace eyestalk ablation, with the aim of making seed production more efficient and animal-friendly. In order to develop a new maturation promoting technology that can replace eyestalk ablation, RNA interference is used here to suppress *VIH* gene expression, and thus decrease the synthesis of endogenous VIH.

In *Litopenaeus vannamei*, seven peptides (sinus gland peptides: SGP-A to -G) have been previously identified from the sinus glands in the eyestalks. Among these peptides, six peptides (A, B, C, E, F, G) have been demonstrated to possess “VIH” activity; VIH suppresses the synthesis of egg yolk protein. Against this background, we cloned full-length cDNAs from the eyestalks, and also elucidated the gene structure of these five *VIHs* (Fig. 1). Moreover, using this genetic information, we established a quantitative real-time PCR system for multiple *VIHs* in *L. vannamei*, and the expression level of each *VIH* in the eyestalk was determined in relation to molting and eyestalk ablation in separate individuals. For purposes of development of new techniques for the artificial control of ovarian maturation, we utilized RNA interference to suppress *VIH* gene expression. Firstly, double-stranded RNA (dsRNA) for targeting the most abundant *VIH* gene in *L. vannamei* (*SGP-G*) was artificially synthesized. Next, it was injected into female adults (50 - 70 g body weight) at a final concentration of 3 µg per g body weight. As a result, *VIH* gene expression was significantly decreased both 10 and 20 days after VIH-dsRNA injection; however, there were no observed significant differences in the other groups (Fig. 2). *VIH* expression levels could be suppressed to less than 10% of original levels up to 20 days with only a single injection of VIH-dsRNA. Hence, using RNA interference, it has become possible to artificially suppress *VIH* gene expression.

Furthermore, it is possible that by simultaneously administering dsRNA complementary to not only the major *VIH* (*SGP-G*), but also to dsRNAs complementary to several other *VIH* genes, it may be possible to achieve even greater suppression of VIH action. In subsequent applications, we suggest that this technique may be applicable to other penaeid shrimp species that harbor similar amino acid sequences for VIH. We intend to continue this research in order to make possible the establishment of a new shrimp-friendly seed production technology and contribute to the sustainable development of the shrimp aquaculture industry.

(B.J. Kang, M.N. Wilder)

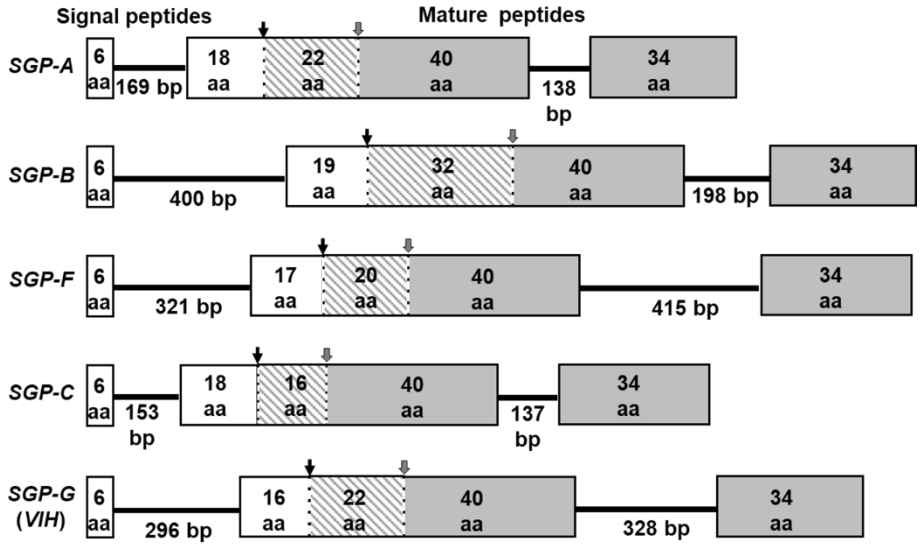

Fig. 1. Schematic diagram of gene structure for *SGPs* having vitellogenesis-inhibiting hormone activity. Exons are indicated as boxes with numbers of amino acid residues (aa), and introns are indicated as bold lines with numbers of base pairs (bp). Reproduced from Kang et al., 2018 with permission from *Fisheries Science*.

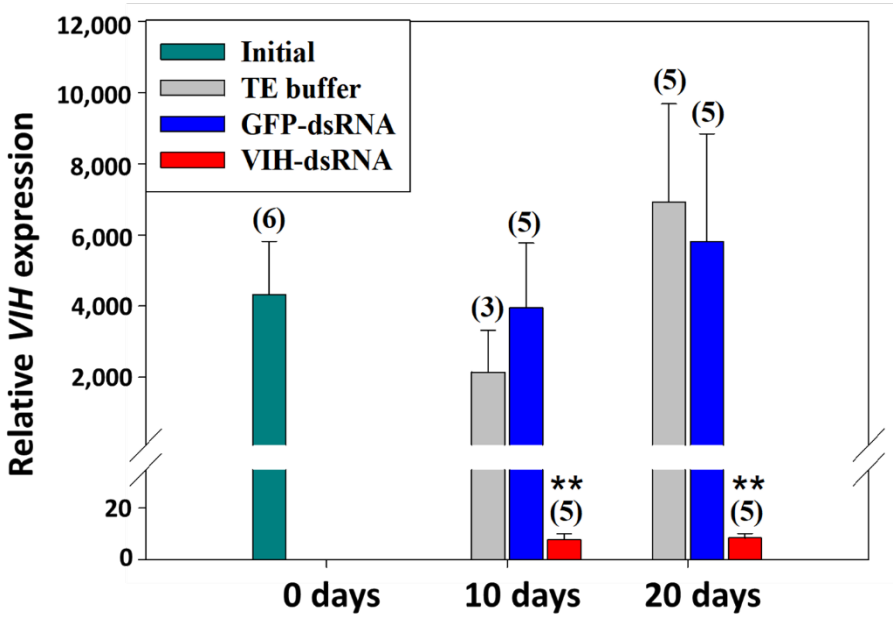

Fig. 2. Suppression of *SGP-G* gene expression following VIH-dsRNA injection. Groups are indicated as follows. Initial: non-treatment; TE buffer: shrimp injected with TE buffer as a vehicle control; GFP-dsRNA: shrimp injected with dsRNA for green fluorescent protein (GFP); and VIH-dsRNA: shrimp injected with VIH-dsRNA. Numbers in parentheses above the bars indicate the number of individuals analyzed. Reproduced from Kang et al., 2019 with permission from *Aquaculture*.

References:

FAO. 2019. *FAO yearbook. Fishery and Aquaculture Statistics 2017/FAO annuaire*. (http://www.fao.org/documents/card/en/c/ca5495t)

Kang BJ et al., 2018. *Fisheries Science*, No84: 649–662.

Kang BJ et al., 2019. *Aquaculture*, No506: 119–126.

Genetic diversity and characteristics of mango genetic resources in Japan

Mango (*Mangifera indica* L.) is one of the major tropical fruits produced and consumed in Japan. Commercial production of mango in the country started in the 1980s mainly in the southwestern region, and substantially by monoculture of the 'Irwin' variety (occupies >90% of production in Japan). Recently, attention has been focused on mango as one of the potential crops for climate change adjustment, and as a premium fruit that can be sold at a high price in commercial markets in Japan. To promote the use of underutilized genetic resources for breeding and/or direct domestic production, assessment of genetic diversity is essential. In this study, we analyzed 120 mango genetic resources conserved at JIRCAS and Okinawa Prefectural Agricultural Research Center, covering almost all mango cultivars in Japan using 46 polymorphic simple sequence repeat (SSR) markers for cultivar identification, genetic relatedness, and genetic diversity.

The 120 mango accessions examined in this study were clearly distinguished into 83 genotypes (cultivars) excluding synonymous and identical accessions by the SSR markers. These 83 cultivars were considered to be representative mango genetic resources possessed in Japan taking their introduction background into account.

Principal coordinate analysis (PCoA), one of the multivariate analyses based on SSR data, indicated that accessions from India had a close relationship with accessions from the USA, while accessions from Thailand, Taiwan, Philippines, and Vietnam seemed to be genetically separate (Fig. 1). These groupings appear to correspond to the previously defined Indian and Southeast Asian types, and suggest that the Florida accessions, which originated from hybrids between those two types, are more closely related to the Indian type.

The accessions that we examined cover almost all mango cultivars in Japan, therefore their genetic information will pave the way to the use of genetic resources for breeding and/or direct domestic production in Japan. In addition, the accessions used in this study, mainly selected and established in Florida, USA, and disseminated to major production countries/areas, have been considered, reflecting the genetic diversity as representative of major cultivars in the world. Therefore, the SSR marker and genotype information in this study are possibly useful for assessing genetic diversity in other countries and areas of mango production.

Information on variety characteristics of 62 cultivars conserved with successful flowering and bearing fruits at JIRCAS-TARF (Ishigaki, Okinawa) were summarized and published on the website titled "JIRCAS Mango Genetic Resources Site" (https://www.jircas.go.jp/ja/database/mango/mango-top) (Fig. 2). This website describes the diversity of mango varieties and characteristics such as flowering period, harvesting time, and fruit quality using the data obtained during the 2010-2011 cultivation period at JIRCAS-TARF.

(S. Yamanaka, T. Ogata, H. Takagi, N. Kozai [Kagoshima University], M. Matsumura [Okinawa Prefectural Agricultural Research Center (OPARC)], Y. Onoue-Makishi [OPARC], N. Urasaki [OPARC], M. Shoda [OPARC], K. Nashima [Nihon University], F. Hosaka [Institute of Fruit Tree and Tree Science, NARO (NIFTS)]), T. Yamamoto [NARO (NIFTS)])

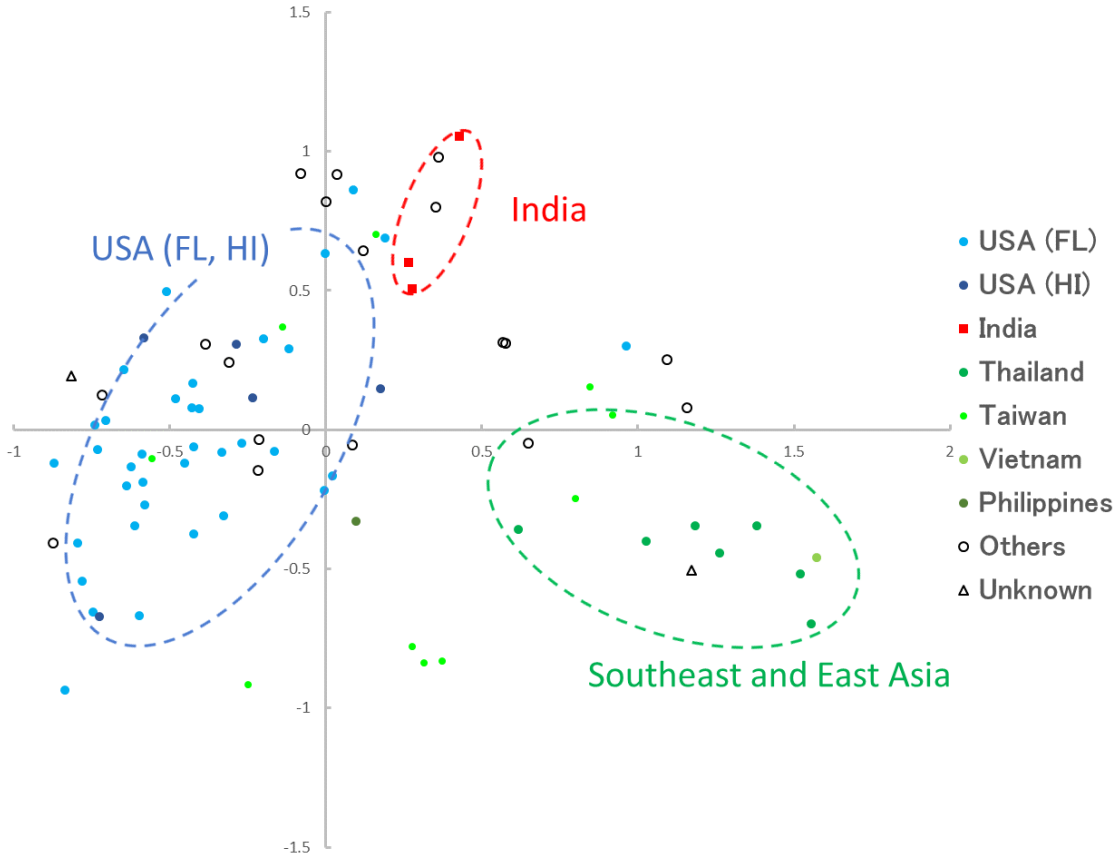

Fig. 1. A scatter plot showing the result of PCoA based on SSR marker analysis for 83 accessions of mango genetic resources in Japan. Three groups based on the origins were found (dotted circles).

Fig. 2. Mango genetic resources conserved at JIRCAS (left), a screenshot of the top page of the “JIRCAS Mango Genetic Resources Site” (center), and a linked page on the website, showing important information on mango variety characteristics (right).